View metadata, citation and similar papers at core.ac.uk

brought to you by CORE

provided by Clemson University: TigerPrints

Clemson University
TigerPrints

All Theses | Theses

5-2014

ADSORPTION OF SYNTHETIC ORGANIC CHEMICALS: A COMPARISON OF SUPERFINE POWDERED ACTIVATED CARBON WITH POWDERED ACTIVATED CARBON

Semra Bakkaloglu
Clemson University, baksemra@gmail.com

Follow this and additional works at: https://tigerprints.clemson.edu/all_theses


Part of the Environmental Engineering Commons, and the Environmental Sciences Commons

Recommended Citation
Bakkaloglu, Semra, "ADSORPTION OF SYNTHETIC ORGANIC CHEMICALS: A COMPARISON OF SUPERFINE POWDERED ACTIVATED CARBON WITH POWDERED ACTIVATED CARBON" (2014). *All Theses*. 1983.
https://tigerprints.clemson.edu/all_theses/1983

This Thesis is brought to you for free and open access by the Theses at TigerPrints. It has been accepted for inclusion in All Theses by an authorized administrator of TigerPrints. For more information, please contact kokeefe@clemson.edu.

ADSORPTION OF SYNTHETIC ORGANIC CHEMICALS: A COMPARISON OF SUPERFINE POWDERED ACTIVATED CARBON WITH POWDERED ACTIVATED CARBON

A Thesis

Presented to

the Graduate School of

Clemson University

In Partial Fulfillment

of the Requirements for the Degree

Master of Science

Environmental Engineering and Science

---

by

Semra Bakkaloglu

May 2014

Accepted by:

Dr. Tanju Karanfil, Committee Chair

Dr. David Ladner

Dr. Cindy Lee

ABSTRACT

In literature, manufacturer-supplied powdered activated carbon has been ground to produce submicron particles with mean diameter lower than 1μm for use as an adsorbent during water treatment. Superfine powdered activated carbon (SPAC) can be used for removal of natural organic matter as well as synthetic organic chemicals (SOCs) from water. It has been suggested that SPAC has higher adsorption capacity than powdered activated carbon (PAC) due to larger external surface area and mesopore volume. Another advantage of SPAC over PAC is the faster uptake rate for both NOM and SOC during adsorption owing to small particle size. Therefore, understanding SPAC adsorption capacity and kinetics on NOM and SOC is crucial for future studies and usage of it.

The main objectives of this study were to: (i) understand the impact of crushing on carbon characteristics; (ii) investigate the SPAC adsorption capacity and rate for selected SOCs in distilled and deionized water (DDW) and natural waters from Myrtle Beach, South Carolina, and compare with PAC adsorption; (iii) evaluate adsorption mechanism of four SOCs, phenanthrene (PNT), atrazine (ATZ) , carbamazepine (CMZ) and 2-phenylphenol (2PP), with different properties planarity, polarity, and hydrogen/electron donor/acceptor ability on SPAC and PAC.

One commercial PAC and its SPAC form created using a special mill were used in the study. Isotherm and kinetic experiments were performed in five different waters: DDW, diluted Edisto raw river (DOC=4mg/L), diluted Myrtle Beach raw waters

(DOC=4mg/L and 10 mg/L) and Myrtle Beach treated (after conventional treatment) water (DOC=4 mg/L). One week and six hours contact times were used for the isotherm and kinetic experiments.

First, the role of carbon characteristics on the adsorption was examined. The characterization of SPAC and PAC samples showed that the crushing process caused some changes in the pore volume distribution and surface acidity of the activated carbon. After pulverization, the pore volume distribution was mainly formed by mesopore and macropore region rather than micropore region. Carbon blending caused an increase of iron, nitrogen and oxygen content. The oxidation of surfaces and pH_{PZC} values were decreased.

Then, the SPAC and PAC adsorption capacity and rate for selected SOCs in distilled and deionized water (DDW) and natural waters from Myrtle Beach were investigated. The isotherm results showed that all PAC adsorption capacities were higher than SPAC. However for adsorption kinetics, SPAC exhibited faster uptakes for PNT, ATZ and CMZ in all background solution than PAC did. On the other hand, SPAC was not advantageous for 2PP compared to PAC in both DDW and natural waters. That may result from multiple factors: (i) higher solubility of 2 PP, (ii) the larger third dimension as compared to other molecules, and (iii) the presence of an electron donating (-OH) group on its structure, which makes the molecule slightly negative charge and cause the deduction in interaction with SPAC whose surface is slightly higher negatively charged. The presence of NOM had a small impact on the adsorption rates of four SOCs by SPAC

during the first six hours contact time. The difference in the NOM characteristics (MB raw $SUVA_{254}$=4.4 and MB treated $SUVA_{254}$=2.1, Edisto $SUVA_{254}$=2) and NOM concentrations (4 mg/L vs. 10 mg/L) did not significantly impact the adsorption rates. The only exception was observed for atrazine.

In summary, these findings indicated that the advantage of using SPAC over PAC at the short contact time can be compound specific; on the other hand, SPAC loses its advantages for small molecular weight compounds at equilibrium conditions.

DEDICATION

I would like to dedicate this thesis to especially my mother, Nermin, father, Ismail, and my sisters, Eda and Esra, my grandparents, nephews and all rest of my family for their encouragement and support.

ACKNOWLEDGEMENTS

First and foremost, I thank Allah (God) for giving me the life, the health and the strength to complete this work.

I would like to thank Dr. Karanfil for allowing me the opportunity to work on this project as well as for his constant and thorough guidance. Dr. Karanfil is not only my advisor but also a father figure that I look up to for inspiration and have immense respect for, I could not have asked for a better mentor in my graduate school work. I would also like to thank Dr. David Ladner who is not only my committee member but also my co advisor in this project for his guidance and support. I would like to express my sincere to my other committee member Dr. Cindy Lee for her insight and expertise.

I am grateful to Anne Cummings for her immense patience and help in tracking the problems with machines in the lab. I am also thankful to Onur Apul for his comments, guidance, expertise and revising my work. I would like to thank Mahmut Ersan and Kathleen Davis for their help in the lab especially for carbon characterization and SEM images. I am also thankful to Gamze Ersan and Mengfei Li for being generous to share their lab skill with me. Also, special thanks go to Meric Selbes for being there and always taking special care of me like only he can. He is a wonderful person and a special friend, he is the 'heart' of the research lab. Also, I am thankful to my dear friend Aylin Huylu for her supports. She is one person who will forever be close to my heart.

I would like to acknowledge the Fulbright for funding Master education in US. This is priceless experience for me to be part of Fulbright family. This work was also partly supported by a research grant from National Science Foundation (CBET 1236070).

Special thanks to my friends for making Clemson feel more like home, Tugba Demir, Ayse Korucu, Guliz Coskun, Sevda Sari, Ozgun Ozdemir, Ferhat Bayram, Ercan Dede, Dr.Fehime Vatansever, Alex Haluska, Kata Tisza, Wilson Beita, Dr. Ozge Yilmaz, Samet Bila, Habibullah Uzun, Aslican Yilmaz.

Finally, I am thankful to my parents, grandparents and my sisters for their unconditional love and understanding. Also, I am obliged to brother in law, Ahmet Calikoglu for his boundless helps. Without his support I would have never come this far. I am also grateful to my best friends, Meltem Yavuz, Ceyhun Karasayar, Ceren Gursen, Gozde Nazlim, Fulya Akat, Sinem Kaymak, Aysegul Hisar, Hasmet Yaltirak, Ilkay Ihsan Onal for their love and encouragements.

TABLE OF CONTENTS

Table of Contents (Continued)

Page

LIST OF TABLES

LIST OF FIGURES

List of Figures (Continued)

List of Figures (Continued)

List of Figures (Continued)

LIST OF SYMBOLS AND ABBREVIATIONS

Greek Symbols

π	Pi
σ	Sigma
ρ	Dimensionless Parameter
δ	Penetration Depth

Abbreviations

2PP	2 Phenylphenol
AC	Activated Carbon
ATZ	Atrazine
BC	Black Carbon
BET	Brunauer-Emmett-Teller equation
BPKM	Branched Pore Kinetic Model
C	Elemental Carbon
CMZ	Carbamazepine
CO_2	Carbon dioxide
DDW	Distilled and Deionized Water
DOC	Dissolved Organic Carbon
DFT	Density Functional Theory
EDA	Electron Donor Acceptor

List of Symbols and Abbreviations (Continued)

FE-SEM/EDXS	Field emission-scanning electroscopy/energy-dispersive X-ray spectrometry
FM	Freundlich Model
GAC	Granular Activated Carbon
HAA	Haloacetic Acid
H-bonding	Hydrogen bonding
HCl	Hydrochloric Acid
HPLC	High Performance Liquid Chromatography
IUPAC	International Union of Pure and Applied Chemistry
K_{OW}	Octanol-Water Partitioning Coefficient
LM	Langmuir Model
MB	Myrtle Beach
MIB	2-Methylisoborneol
N	Elemental Nitrogen
NaCl	Sodium Chloride
NaOH	Sodium Hydroxide
NOM	Natural Organic Matter
O	Elemental Oxygen
OH	Hydroxide
PAC	Powdered Activated Carbon
PCB	Polychlorinated Biphenyl
PEG	Polyethylene Glycols

List of Symbols and Abbreviations (Continued)

pH	$-\log[H^+]$
pH_{pzc}	pH of point of zero charge
pK_a	$-\log[K_a]$
PNT	Phenanthrene
PMM	Polanyi-Manes Models
PSD	Pore Size Distribution
PSS	Polystyrene Sulfonates
SAM	Shell Adsorption Model
SEM	Scanning Electron Microscopy
SUVA	Specific Ultraviolet Absorbance
SOC	Synthetic Organic Chemical
SPAC	Superfine Powdered Activated Carbon
S_{BET}	Specific Surface Area Obtained from BET Model
S_{ext}	External Specific Surface Area
THM	Trihalomethane
USEPA	United States Environmental Protection Agency
V_{micro}	Micropore volume
V_{total}	Votal pore volume

CHAPTER 1

1 INTRODUCTION

Synthetic organic chemicals (SOCs) are discharged into the environment due to domestic and industrial usage and immense quantities of organic compound production. The effects of exposure to SOC on human health include damage to the nervous system, liver, and kidney, as well as carcinogenicity. For example it has been reported that the phenolic compounds, such as 2-phenylphenol (2PP) can cause cardiovascular system and serious mucosal alteration in sensitive cellular membranes [1]. Moreover, extended exposure to pharmaceutical SOCs may cause adverse effects in both wildlife and human beings, such as prevalent atrazine (ATZ) exposure, which may adversely affect the cardiovascular system, and normal hormone production [2]. Carbamazepine (CMZ) has the potential to increase cancer risk [3]. The Clean Water Act and its amendments have been promulgated by the United States Environmental Protection Agency (USEPA) after detection of these compounds in water body. After, the Safe Drinking Water Act [4] and its amendments were promulgated so as to protect the public from exposure to some of those detrimental and undesirable chemicals. To date, USEPA has set standards for approximately 90 SOCs in drinking water as priority pollutants [5].

Activated carbon adsorption was designated as one of the "Best Available Technologies" to remove SOCs from water [4]. Activated carbon (AC) is defined as "a porous carbon material, a char, which has been subjected to reaction with gases,

sometimes with the addition of chemicals before, during, or after carbonization to increase its adsorptive properties" by the International Union of Pure and Applied Chemistry (IUPAC) [6]. ACs typically have a high degree of porosity and surface areas (e.g., 800-1000 m^2/g) and mainly consist of carbon and other elements such as oxygen, hydrogen, and nitrogen and some other inorganic components.

Activated carbon can be applied in granular and powdered forms. Granular activated carbon (GAC) has the largerest particle sizes ranging from 0.2 to 5 mm, while PAC is pulverized form of GAC with a size predominantly less than 0.1 mm (US Mesh 80) [7, 8]. Moreover, superfine powdered activated carbon (SPAC) is a newly defined form of PAC produced by grinding the PAC into submicron size (<1 micron) [9]. Faster adsorption kinetics, and better adsorption capacity are cited as the main motivation for the application of SPAC in water treatment [10]. But, further researches are necessary to fully understand the SPAC adsorption mechanism.

In literature, the main motivation of using SPAC is to provide greater adsorption capacity of naturally occurring organic matter [11], which is ubiquitous in fresh water supplies [12]. NOM is composed of a heterogeneous mixture of humic substances, hydrophilic acids, proteins, lipids, carbohydrates, carboxylic acids, amino acids, and hydrocarbons [13]. Also, it has been shown that NOM hinders synthetic organic chemicals adsorption activated carbon surface through site competition and/or pore blockage mechanisms [14, 15].

In previous studies, SPAC was mainly examined for adsorption of NOM, a few SOCs such as atrazine and methylene and small molecules caused taste and odor problem in water systems such as blue 2-methylisoborneol (MIB) and geosmin [10, 16]. Understanding SPAC adsorption for various SOCs is crucial to predict SPAC behavior in different environmental systems. Our interest in this study stems from the realization of the lack of information of adsorption on different SOCs on SPAC. The main motivation for this thesis research was to improve the understanding of SPAC characteristics, adsorption mechanism and factors controlling the adsorption of four SOCs (PNT, ATZ, CMZ and 2PP) with different planarity, polarity, and hydrogen/electron donor/acceptor abilities.

CHAPTER 2

2 LITERATURE REVIEW

2.1 Activated Carbon

ACs are carbonaceous materials which have been widely used in pollution control systems owing to their high adsorption capacities. Application of PAC in water treatment has limited removal efficiency due to limited contact time with PAC and SOCs in water system. Longer contact time is necessary to fully utilize the capacity of PAC. That problem can be solved by reducing PAC particle size, thus increasing the adsorption kinetics [9]. According to Matsui [9], SPAC removed contaminants with a lower dosage and shorter contact time than is the case of PAC adsorption during pretreatment.

2.1.1 Origins and Productions of Activated Carbon

Many carbonaceous materials such as coal, wood, lignite, fruit seeds, petroleum coke and coconut shells can be converted to activated carbon. These materials have high carbon content, low inorganic content and they are relatively inexpensive [17].

Carbonization includes a series of reactions for the pyrolysis of organic material to elemental carbon. The char is then “activated” by thermal or chemical mechanisms, though a combination of the two may be employed to achieve a desirable level of porosity [18]. Thermal activation is a two steps process. At medium and high temperature, raw material is carbonized. After carbonization process in the presence of

inert gas, char rich carbon is partially gasified in direct fired furnaces by high temperature by an oxidizing agent such as carbon dioxide, air, or steam to create a porous structure. On the other hand, chemical activation is a single step carbonization process. The raw material is impregnated at high temperatures with chemical agents such as zinc chloride, phosphoric acid and alkali chemicals. After carbonization, the impregnated product is completely washed to remove the surplus activation agent [19]. Generally, compared to physical activation, chemical activation can remove the heteroatoms like hydrogen and oxygen at lower temperature and obtain greater yield owing to low activation temperature and cross linking reaction [19].

2.1.2 Structure of Activated Carbon

Activated carbons have a microcrystalline structure, which is rigidly interconnected and consist of a stack of graphitic planes. Graphite is a layered structure in the atoms of carbon bonded by σ- and π- bonds to three neighboring carbon atoms. As seen in Figure 2.1, graphite planes have a parallel alignment maintained by dispersive and van der Waals forces. The interlayer spacing of activated carbon microcrystalline structure is 0.335 nm, which differs from graphite, which has interlayer spacing between 0.34 and 0.35 nm [20].

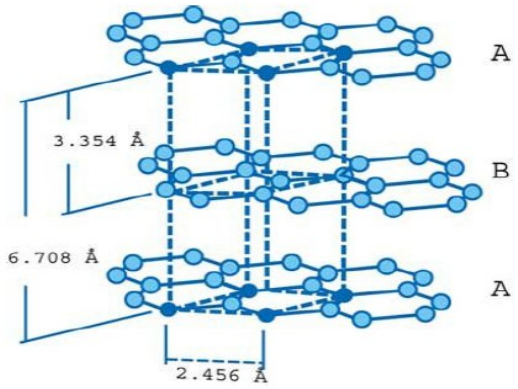

Figure 2.1 Structure of graphite crystal [21]

Activated carbon pore sizes start from less than one nanometer to several thousand nanometers. Pore sizes are classified based on their width (w) which is the distance between the walls of a slit-shaped pore or the radius of a cylindrical pore [20]. According to IUPAC recommendations, pores of adsorbent are classified into four groups, (1) Macropores with a pore width larger than 500 Å, (2) Mesopores with widths from 20 to 500 Å, (3) Secondary micropores with widths from 8 to 20 Å, and (4) Primary micropores with a pore width less than 8 Å [22, 23]. The adsorbent particle size distribution determines the fraction of the total pore volume that can be accessed by an adsorbate of a given size. Figure 2.2 shows the illustration of pores on GAC.

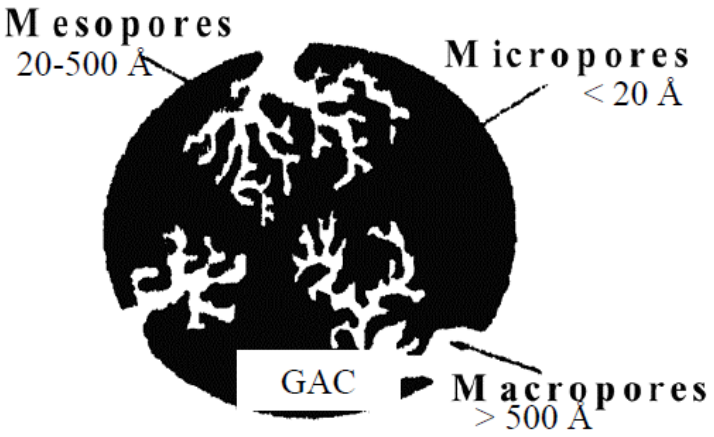

Figure 2.2 Schematic pore structure of GAC [24]

Generally, ACs are described by polydisperse capillary structures consisting of various pore size and shapes. There are several methods to describe pore shape such as ink-bottle shape, regular slit-shaped et all. to [20].

AC includes several heteroatoms based on the original material, such as oxygen, hydrogen, nitrogen, sulfur and phosphorus, and they are chemically connected to the carbon surface during the synthesis process, forming carbon-heteroatom structures [25]. Some ACs can also contains different amounts of inorganic matter (ash content) depending on the nature of raw material.

2.1.3 Applications of Activated Carbon

Large internal surface area and porosity of ACs allow them to adsorb various pollutants; therefore, they can be used in various applications. For example, AC is

primarily found in household filters for faucets and cigarette fibers. In industry, it is generally used for purification in refineries and as a catalyst. Specifically, ACs are used in the production of high purity water in manufacturing of electronics; hospitals and medical laboratories; industrial and domestic wastewater treatment; municipal water filtration; solvent recovery; and removal of color, odor or taste [26, 27]. Water treatment covers more than half of its usage in United States. It is generally applied for organic pollutant removal from drinking water, although it might be implemented for odor, taste and color refinement as well [18].

2.2 Superfine Powdered Activated Carbon

PAC is one of the best available technologies to remove dissolved contaminants such as NOM, small molecular weights compounds and SOCs from water resources; however, the residence time at water treatment plants is shorter than the amount of time needed to ensure the full utilization of maximum PAC adsorption capacity. This insufficient contact time of PAC with target compounds causes the waste of PAC and consequently higher treatment costs. A large PAC-water reactor might be a solution, but it would limit the benefit of the small footprint of membrane filtration equipment. Another strategy is to use smaller PAC particles to provide faster adsorption kinetics [28]. Recently, Matsui et al. [9, 29, 30] have proposed the application of an extremely small, micro-ground PAC, which is SPAC whose particle size is less than 1 μm.

Generally, the particle size effect with the smaller porous adsorbent is explained by the shorter distance from the external surface of particle to its inside and the higher external particle surface area per unit mass for SPAC. Therefore, it is reported that SPAC has superior qualities over PAC for both improvement of uptake rate and increase of adsorption capacity of dissolved organic compound and trace organic contaminants. In fact, it is recently being used in membrane process not only as coating material but also as pretreatment [30, 31].

2.2.1 Adsorption Capacity of SPAC

In literature, SPAC adsorption capacity on NOM, small molecular weight compound such as geosmin and MIB, and some SOCs were investigated. It is stated that SPAC has higher adsorption capacity than PAC due not only to the specific surface area increase [10] but also higher mesopore volume [32]. Generally, it is deemed that the advantage of the high adsorption capacity of SPAC is more important for adsorbing high molecular weight compounds such as NOM. Although there is limited information about the mechanism of increasing adsorption capacity owing to the decrease in the particle size with respect to adsorbate property, some arguments about SPAC adsorption capacity on both NOM and SOCs are studied in this part.

Most studies have sought to answer the question: why SPAC has more NOM adsorption capacity than PAC? First, Matsui and coworkers [33] proposed that the reason for the increase in adsorption capacity on SPAC is due to higher mesopore volume. By

grinding, accessibility of pores increases due to fraction of ink-bottle constrictions in the internal pores of activated carbon particles [28]. These fractures occurred at constricted pathways to enlarge the interior pores, which make them accessible by large target compounds. After fracturing, an increase in the interior pores provides the enlargement of total surface area of larger pores. Therefore, on the basis of this ink-bottle fracture hypothesis, it is expected that micropore volume decreases, mesopore and macropore volume increase. However, Matsui and coworkers [10] changed their position by using external surface area increment rather than increase in mesopore volume to explain enlargement of adsorption capacity when particle size gets smaller. Ando [10] have reported that there are less pore size distribution differences between the SPAC and PAC particles that they used. Thus, Matsui and co-workers [10] speculated that raising the SPAC adsorption capacity for NOM originated from the increase in surface area of the SPAC particles. They reported that adsorption occurs mainly at the external region of the SPAC particles with little penetration into the adsorbent particle [10]. Second, Ellerie [34] reported that after crushing, pore volume distribution was mainly consisted of mesopore and macropore volume. In experiments by Ellerie [34], SPAC presented higher mesopore volume and lower micropore volume than PAC demonstrating better adsorption capacity for methylene blue. Also, Knappe and co-workers [32] have still suggested that SPAC has much more NOM adsorption capacity because of the increase in the mesopore volume as Ellerie [33] did. So, even if some SPAC particles show slight

differences on pore size distribution than PAC particles, some of them do not demonstrate variations in pore size distribution.

SPAC adsorption capacity on the NOM was mainly investigated in literature. The larger molecular weight of NOM has more adsorption affinity to SPAC than PAC [10, 32, 33, 35]. To clarify the effect of size of on NOM adsorption capacity for SPAC, polystyrene sulfonates (PSSs) and polyethylene glycols (PEGs) were examined. As the molecular weights of PSS increase, the difference in the adsorption capacities between SPAC and PAC increases because larger particle has lower saturation rate. Moreover, if NOM has higher SUVA values i.e. more aromatic and conjugated double bond structure, then there is a greater gap between adsorptions of SPAC and PAC [10]. The difference in the amount of NOM adsorption between SPAC and PAC decrease slightly at lower MW of NOM. It is deemed that NOM and PSS aggregate in the vicinity of the outer region of carbon particles and they can diffuse to certain into the interior of AC particles after reaching equilibrium. In other words, because NOM is adsorbed and aggregated mainly in the shell region close to the external surface of particles, NOM does not fully penetrate through carbon particles [10, 36, 37]. Therefore, higher specific external surface area of SPAC ensures larger NOM adsorption capacity than PAC.

In addition to studies about NOM adsorption capacity on SPAC, small molecular weight compounds and some SOCs adsorption capacities were also studied. According to Matsui et al. [33], although micro-grounded PAC showed better NOM and PSS (1.8k) removal than PAC, this is not always valid for micromolecules, such as phenol. For AC,

it was previously reported that the adsorption capacity of pure, low molecular weight chemicals do not depend on the pulverization of activated carbon or a particle size of carbon [33, 38].

The literature regarding the adsorption of small molecular weight compounds and SOCs by SPAC are not very board especially when compared to NOM adsorption by SPAC. Generally, small compounds 2-methylisoborneol (MIB) and geosmin have been studied in order to understand the SPAC adsorption mechanism. It was stated that MIB and geosmin adsorption capacities on SPAC is similar to PAC in both distilled and deionized water and under NOM competition [16, 39]. Grinding did not increase efficiently the MIB, and geosmin removal efficiency from water. To be more specific, SPAC adsorption capacities was higher 20 % of MIB and 23% of geosmin in organic free water than PAC adsorption capacity. On the other hand, methylene blue showed higher adsorption affinity on SPAC than PAC [31]. However, in the same study atrazine showed higher affinity on PAC than SPAC.

2.2.1.1 Modeling of SPAC Adsorption Capacity

Adsorption isotherms can be modelled by Freundlich or Langmuir isotherms. These equations assume that adsorption capacity is independent of the adsorbent particle size. Matsui et al. [36] modified the Freundlich isotherm (Eq. 2.1) so as to describe adsorption capacity changes with respect to adsorbent particle size. They assumed that K, parameter of adsorption capacity, increased with decreasing distance from the adsorbent

particle surface, which is the function of radial distance and particle radius [36], as follows:

$$q_E = KC_E^{1/n} \tag{2.1}$$

where C_E is the liquid-phase concentration (mg/L), q_E is the amount adsorbed in solid-phase in equilibrium with liquid-phase concentration (mg/g), *n* is the Freundlich exponent *and K* is the Freundlich adsorption capacity parameter (mg/g)/(mg/L)$^{1/}n$. By using radial coordinates, the Freundlich adsorption capacity parameter is a function of particle radius and radial distance; adsorption capacity of an adsorbent with respect to radius *R* at radial distance *r* is then given by Eq. (2.2), as follows [36]:

$$q_S(r,R) = K_S(r,R)\, C_E^{1/n} \tag{2.2}$$

here *R* is the adsorbent particle radius (μm), *r* is the radial distance from the center of a PAC particle (μm), $q_S(r, R)$ is the local solid-phase concentration (mg/g) at radial distance *r* in an adsorbent with radius *R*, and $K_S(r, R)$ is the radially changing Freundlich adsorption capacity parameter (mg/g)/(mg/L)$^{1/n}$ as a function of adsorbent radius *R* and radial distance *r*. PAC and the SPAC particles are assumed to spherical shape [36].

Finally, adsorption capacity of an adsorbent with the particle radius R in the equilibrium with liquid phase concentration C_E is given by Eq.(2.3), as shown in below [36]:

$$\int_0^R q_S(r,R)\, \frac{3r^2}{R^3}\, dr = C_E^{1/n}\, \frac{3}{R^3} \int_0^R K_S(r.R) r^2 dr \tag{2.3}$$

If the adsorbent size is not uniform, adsorbent adsorption capacity becomes Eq. (2.4) [36]:

$$q_E(r,R) = C_E^{1/n} \frac{3}{R^3} \int_0^{\infty} [\int_0^{R} K_S(r.R) r^2 dr] \, f_R(r) dr \quad (2.4)$$

where $f_R(R)$ is the normalized particle size distribution function of adsorbent (μm^{-1}) and q_E is the overall adsorption capacity of adsorbent (mg/g).

$K_S(r,R)$ equations are modelled in Eq. (2.5)to determine if K decreases linearly with the increasing distance from external surface to depth, δ, some of the adsorption capacity remains subsequently at a level, p, inward from that depth, as depicted in Figure 2.3 [36].

$$K_S(r,R) = K_0 [\max (\frac{r-R+\delta}{\delta} ,0)(1- p)+ p] \quad (2.5)$$

where δ is thickness of the penetration shell (or the penetration depth, μm), K_0 is the Freundlich parameter of adsorption at the external particle surface $(mg/g)/(mg/L)^{1/n}$), and p is a dimensionless parameter which defines availability of internal porous structures for adsorption [36].

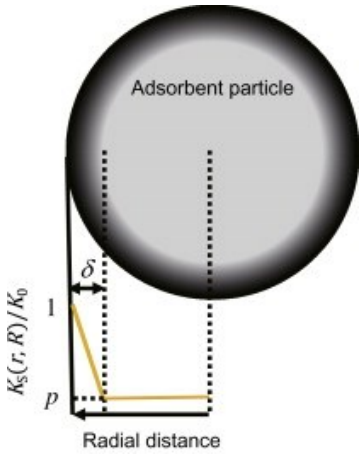

Figure 2.3 Adsorbent particle regions to be used in SAM [36]

According to Figure 2.3 and modeling equations, some of the interior region of adsorbent particles is available for adsorption; therefore, when some molecules adsorb onto the outer region which is close to the particle surface, shell region, the other molecules probably diffuse into and adsorb inner region of activated carbon particles. Shell Adsorption Model [40] is introduced for the adsorption capacity of superfine powdered activated carbons in Eq. (2.6) [36].

$$q_E(r,R) = C_E^{1/n}\frac{3K_0}{R^3}\int_0^{\infty}\{[\int_0^{R}[\max(\frac{r-R+\delta}{\delta},0)(1-p)+p]r^2dr\}f_R(r)dr \quad (2.6)$$

According to Matsui and co-workers [36], SAM equations can be used for PSS adsorption capacity on SPACs. To elucidate the SAM model, Ando et al. [37] observed the solid phase adsorbate concentration profile of PAC particles by field emission-scanning electroscopy/energy-dispersive X-ray spectrometry, FE-SEM/EDXS, and thus they verified the shell adsorption mechanisms.

2.2.2 Adsorption Uptake Rate of SPAC

As opposed to the minor advantage of SPAC over PAC in adsorption capacity, SPAC accelerates the uptake rate of the adsorption of contaminant compounds [41] due to smaller particle size [32-34].

In contrast to the adsorption equilibrium, SPAC and PAC adsorption kinetics are different even for small compounds. SPAC adsorption kinetics are much faster than PAC particles in both NOM solution and DDW. The faster uptake rate of SPAC is more evident when SPAC is coated on membranes [42] due to the short contact time with higher feed concentration.

According to Knappe et al. [33], SPAC uptake rate of NOM is faster than parent PAC. SPAC can reach 80% (by UV_{260}) and 60% (by TOC) of the adsorption equilibrium within 1 minute of contact time, whereas PAC reaches only less than 50% (by TOC) of the adsorption equilibrium in the same time [33]. It takes 6.3 minutes to reach NOM adsorption to equilibrium for PAC particles [30].

For small molecules and SOCs, the adsorption kinetics of SPAC and PAC are quite different, in contrast to adsorption capacities on SPAC and PAC. In literature, SPAC adsorption rate is superior to PAC under every condition studied for geosmin, MIB, THM precursor, HAA precursor, PFCs, methylene blue and atrazine removal [34, 43, 44] because of its smaller particle size and larger mesopore volume, which aid the movement of micropollutants into the carbon pore matrix [32]. For example, at the same

dosage for SPAC and PAC, 90% of geosmin removal was obtained within 30 minutes for SPAC adsorption, although PAC adsorption reached up to 30% of geosmin removal at the same point [45]. Also, SPAC removed THM and HAA precursor two times more than PAC in 60 minutes of contact time [32]. Furthermore, 20 mg/L of SPAC showed better removal of atrazine achieving 98% removal compared with 65% with 70mg/l of PAC without competitive adsorption after one hour [43]. Also, even the same dose was applied for PAC and SPAC for atrazine removal, without competitive adsorption then SPAC show fast adsorption kinetics.

2.2.2.1 Modeling of SPAC Uptake Rate

Kinetic models have successfully predicted numerous batch reactor adsorbate concentration profiles and provided significant insights on the way adsorbents function. Uptake rate of particle depends the rate of external mass transfer and intra-particle transport. Thus, the rate of adsorption in porous adsorbents is controlled by pore network transport. This intra-particle diffusion may occur by several different mechanisms depending on the pore size, the adsorbate concentration and other conditions. The internal diffusion for an activated carbon in an aqueous system can be described as surface diffusion, pore diffusion and/or a combination of surface and pore diffusion [46].

In literature, the adsorption model for the uptake rate of SPAC particles with respect to their particle size, homogeneous surface diffusion model (HSDM) and branched pore kinetic model (BPKM) has been evaluated, then Matsui and his client

decided to modify BPKM with SAM to understand kinetics of SPAC particles behavior [45].

HSDM is a traditional method to predict kinetics of the adsorption process. Internal diffusivity is considered to be constant in that model. It is assumed that spherical particle of a porous adsorbent is consisted of uniformly distributed micropores, which branch off macropores undergoing radial mass transport [28, 45]. If the HSDM is not modified to vary surface diffusivity based on changes in carbon particle size, the model does not accurately describe the SOC adsorption on different particle size adsorbents [44].

Also, the branched pore kinetic model (or the multi-pore model) [46, 47] has been widely used to determine adsorption parameters and kinetics in liquid phase adsorption studies by activated carbons. The BPKM describes the mass transfer mechanism in adsorption by three processes: one is the external mass transfer rate across the liquid film of the carbon particle, second is the the radial intraparticle diffusion through macropore to micropore, and third is the local diffusion from macropore to micropore [45].

For HSDM, it is assumed that radial diffusion is the sole rate limiting step in mass transfer resistance; however, in addition to radial diffusion, BPKM also asserts local micropore diffusion. Based on simulation of kinetic data of geosmin with both HSDM and BPKM, it was assumed that when the particle size decreases from PAC to SPAC, overall mass transfer process shifts from radial intraparticle diffusion to local micropore

diffusion because the intraparticle surface diffusivity [48]. SPAC surface diffusivity was lower than that PAC in HSDM. On the other hand, rate coefficient for mass transfer between macropore to micropore (k_B) values is more significant during SPAC adsorption process in BPKM. Therefore, the BPKM successfully described the geosmin adsorption on SPAC and PAC [45].

Moreover, BPKM was modified by incorporating SAM to describe the local adsorption equilibrium in internal pores of activated carbon particle, because the interior of the activated carbon particle is not homogenous and BPKM assumed radial intraparticle diffusion through macropores in an adsorbed state. Matsui research group has modeled diffusion of molecules in liquid-filled macropores (pore diffusion) instead of adsorbed state diffusion in Eq. (2.7)[45].

$$\phi \frac{\partial q_M(t,rR)}{\partial t} = \frac{\phi D_p}{\rho r^2} \frac{\partial}{\partial r} \left(r^2 \frac{\partial C_M(t,r,R)}{\partial r}\right) - k_B[q_M(t,r,R) - q_B(t,r,R)] \quad (2.7)$$

Where c_M (t, r, R) is the liquid-phase concentration in a macropore of an adsorbent of radius R; at radial distance r and time t (ng/L); q_M (t, r, R) is the solid-phase concentration in a macropore of an adsorbent of radius R, at radial distance r and time t (ng/g); q_B (t, r, R) is the solid-phase concentration in a micropore of an adsorbent of radius R, radial distance r and time t (ng/g); t is the time of adsorption (s); ϕ is the dimensionless of fraction of adsorptive capacity in the macropore region; ρ is the adsorbent density (g/L); D_P is the diffusion coefficient in the macropore (cm^2/s); and k_B is the rate coefficient for mass transfer between macropores and micropores (s^{-1}) [45].

Also, according to Matsui et al. [49] the local adsorption equilibrium was defined as follows:

$$C_M(t,r,R) = \left(\frac{q_M(t,r,r)}{K_S(r,R)} \right)^n \quad (2.8)$$

Because model simulations of both MIB and geosmin concentrations were successful in describing kinetics behavior, these equations can evaluate the impact of carbon particle size on the concentrations of SOC remaining after a given contact time.

2.2.3 Effect of SPAC Properties on Adsorption

There are limited numbers of studies that have studied on the role of physical factors of SPAC, such as surface area, particle size, pore size distribution of the activated carbon particles. Therefore, besides the chemical interactions involved in the adsorption of SOCs, a fundamental understanding of the physical factors of ACs is crucial to predict the fate and transport of SOCs in the environment.

2.2.3.1 Surface Area and Particle Size

When the particle size decreased, the specific external surface area of the superfine powdered activated carbons become larger, which enhance the NOM adsorption capacity [10, 32, 39]; even though it has been suggested that BET surface area is a poor indicator of capacity of adsorbent to remove organic micropollutants from natural water [50]. There was no common trend between the increases in Brunauer–Emmett–Teller (BET) surface area by decreasing particle size. Some authors assumed

that SPAC particles had more BET surface area than PAC particles [44]; however, the PAC particles had larger BET surface areas than SPAC particles as reported in Ellerie's study [31].

Also, micropores pore volume with widths corresponding to about 1.3 to 1.8 times the kinetic diameter of the adsorbate controlled the adsorption capacity [51]. But, that claim has not been further studied by different micromolecules adsorbed on various pore sized SPAC particles.

On the other hand, the adsorption rate improved with smaller particle size due to decrease in the travel distance for intraparticle radial diffusion and larger specific surface area per adsorbent mass. When considering the adsorbent particle size effect on removal efficiency, internal diffusivity cannot be ignored. It should be noted that internal diffusivity decreases as the particle size decreases; therefore, the improvement of the overall adsorption rate with smaller PAC particles might be reduced to some extent owing to lower internal diffusion rate [45]. It was deemed that decrease in the particle size increased the adsorption kinetics. Contrary, blending of carbons would not offer advantages for the removal of PFCs even if MWs rangef from 200 to 500 Da [48].

Matsui et al. [49] evaluated the optimum particle size diameter, which best describes the entire size distribution of any given carbon sample for adsorption kinetics, by using BPKM and SAM simulations. They worked with MIB and geosmin adsorption on three adsorbates, which have different particle size distribution. They found that D_{40} is

the best characteristic size to represent the kinetics of MIB removal, whereas D_{30} is the best for removal of geosmin, which has slower intraparticle mass transfer rate regardless of the size distribution. Although the grinding type or time caused some variation in size dispersity, they have proposed D_{40} be used as a representative particle diameter in model simulation when a uniform adsorbent particle size is assumed [44].

2.2.3.2 Pore Size Distribution

According to Li et al. [51], the pore size of the adsorbent has an impact on organic contaminant adsorption in two ways. First, decreasing pore size increaes the strength of adsorption process due to not only the increase in the contact points between the adsorbate and the adsorbent surface [15] but also increase the adsorption potential between counter pore walls start to overlap. Second, if the pores are not large enough, size exclusion constrains the adsorption of contaminants of a given size and shape [51].

The pore size distribution (PSD) determines the pore volume accessible to the target. The larger mesopore volume of SPAC boosts adsorption rates beyond those attributable to differences in particle size alone because mesopores can serve as transport pores [32, 34, 48]. However, Aldo et al. [10] have reported that pore size distributions their SPAC and PAC particles does not alter. Therefore, they cannot explain the higher NOM adsorption capacities for SPAC particles by that idea.

2.2.3.3 Surface Chemistry of Carbon

Surface chemistry is related to functional groups that influence the adsorption properties and reactivity of the carbons. Various techniques can be used to alter the surface chemistry of a carbon such as heat treatment, oxidation, amination, and impregnation with various inorganic compounds [52]. By these methods, structural and chemical properties of the carbon can be modified including both electrostatic and dispersive interactions [52, 53]. For example, carbon oxidation decreases both pH_{PZC} and the dispersive adsorption potential by reducing the density of π-electron [26, 53].

Functional groups can alter the acidity or basicity of the carbon surface. Acidity and basicity are determined by oxygen and nitrogen containing surface functional groups, respectively [11]. Acidity and polarity of the surface increase by increasing oxygen-containing functional groups on the carbon surface [52], which caused a decrease in adsorption affinity [25, 51, 54, 55]. For example, the adsorption affinity of phenolic compounds decrease with increasing acidity of the carbon surface [40, 56]. Moreover, surface acidity triggers water adsorption, which decreases the adsorption uptake. Water molecules can adsorb on hydrophilic oxygen groups on carbon surface by hydrogen bonding and causes formation of water clusters [26, 57]. Moreover, Garcia et al. [55] also observed that activated carbon adsorption capacity with low concentrations of surface oxygen groups was higher than high concentrations of surface oxygen groups.

In the SPAC literature, wood-based thermally activated, coal-based chemical and thermal activated and coconut-based were used in the adsorption comparisons of SPAC and PAC particles. Coconut and wood based SPACs had higher adsorption capacity and kinetics than coal based SPAC [10, 32].

2.2.4 Effect of Synthetic Organic Compound Properties

In addition to adsorbent properties, the adsorbate physicochemical properties have important impacts on the adsorption capacity and rate. Although the molecular dimension and conformation dominate pores accessibility, the solubility also identifies the hydrophobic interactions. It has been indicated that when the molecular size gets larger, the adsorption rate constant decreases [58]. Although there is limited research about the effects of the properties of SOCs on their adsorption by SPAC, the influence of those properties can be generally evaluated based on previous research with other activated carbons.

2.2.4.1 Size and Configuration

The dispersive interactions between sorbate and sorbent electron systems and the sorbate-sorbent separation distance (steric effects) are two factors that affect the interaction efficiency between a hydrophobic adsorbate and adsorbent. Cornelissen et al. [59] investigated about black carbon (BC) sorption for planar and nonplanar. They have indicated that steric hindrance rendered the strong, specific BC sorption sites less accessible for nonplanar 2,2′-dichlorobiphenyl (2,2′-PCB) which is too large a molecule

to pass into the majority of narrow BC nanopores, whereas the planar compounds thickness was not greater than the average BC nanopore size [59]. Also, another research among planar and nonplanar PCBs indicated that coplanar PCBs showed greater sorption affinity on the soot materials in comparison with nonplanar congeners because planar compounds have greater ability to approach closely to the flat sorption surface and create favorable π-cloud overlap and increase sorption in narrow pores [60-62].

Furthermore, Guo et al. [63] analyzed the molecular conformation and dimension impact on the adsorption. Three different SOCs, biphenyl, 2-chlorobiphenyl and phenanthrene, with similar physicochemical properties but different molecular conformations were studied by GAC and ACF. Among these three SOCs, biphenyl showed the highest uptake rate and 2-chlorobiphenyl had the lowest uptake rate because of its nonplanar conformation. Although phenanthrene and biphenyl have planar molecular configuration, it appeared that biphenyl accessed and packed in pores more effectively than phenanthrene. Also, smaller width of biphenyl had an advantage of greater accessibility to the pore. Additionally, it was reported that nonplanar molecular conformation alleviates the interactions between adsorbate molecules and carbon surfaces.

2.2.4.2 Hydrophobicity and Polarity

Hydrophobicity can be a driving force for organic compound adsorption on activated carbon. Solubility is a driving force for organic compounds to escape to

interfaces. Most studies have demonstrated that an increase in solubility of SOCs decreases its adsorption on ACs by decreasing its hydrophobicity in the solvent. In other words, adsorption of a hydrophobic compound is energetically more favored than adsorption of a hydrophilic one [26, 51, 64-67].

The polarity of SOC molecules, which originates from electronegativity differences in electronegative ties between the various atoms in a bond, causes an unequal electron density distribution. The adsorption of polar compounds includes specific interactions by oxygen and nitrogen; however, nonpolar molecules are held by dispersive forces [68]. If the compound solubility is reduced, the differences between its polarity and the polarity of the solvent is increased; thus, adsorption of a SOC by AC is increased [69].

The hydrophilic group makes the carbon surface polar, and increases the interactions with polar liquids such as water [68]. The hydrophilic, polar oxygen groups at the entrance of the carbon pores can adsorb water molecules, that interactions drive to formation of water clusters [57]. These clustered water molecules diminishe the accessibility and affinity of organic molecules to the inner pores [26, 65].

2.2.5 SOC-Carbon Interactions

SOC and carbon interactions are controlled by three factors, namely, the physicochemical properties of the AC, the molecular structure of the SOC, and the

solution chemistry. Carbon surface and adsorbates interactions can be physical, chemical and electrostatic interactions.

Physisorption (physical sorption) includes nonspecific interactions that can exist between any kinds of molecules. Physical interactions between aromatic and activated carbon basal planes occur through dispersive interactions in the form of van der Waals interactions [57].

Chemical adsorption (i.e., chemisorption) occurs when an electron is transferred and/or shared between the adsorbate molecules and the carbon surface. Chemical interactions are generally stronger than physical interactions. Chemisorption can include different kind of interactions such as electron donor acceptor interactions between carbon and solute, as well as hydrogen-bonding between the carbon surface with oxygen-containing surface functional groups and similar functional groups of the solute [26, 70].

Another SOC-carbon interaction is the electrostatic interaction between ionic SOCs and charged functional groups on the carbon surface. Dissociation of weak organic acids and bases in solution can affect the adsorption process based on the difference between the pKa of the SOC molecules and the pH of the solution. On the other side, pH_{PZC} indicates the net carbon surface charge. When pH of the solution is higher than pH_{PZC}, the surface charge becomes negative. Therefore, electrostatic attraction or repulsion can occur between the carbon surface and the ionizable SOC based on the pH of the media, pKa of the SOC molecules, and pH_{PZC} of the activated carbon.

2.2.6 NOM Effect on SPAC Adsorption

One of the important factors that affect the removal SOC compounds in the presence of NOM. NOM can significantly reduce the adsorption capacity of a micropollutant; however, a micropollutant does not have an impact on NOM adsorption since NOM can be found at much higher concentration than most of the micropollutants, for instance, MIB, PPCPS (pharmaceutical and personal care products) etc., which occur at ng/L to μg/L levels. The competitive effect causes the reduction of micropollutant adsorption capacity, which depends on the activated carbon pore size [23, 71] as well as the NOM loading on activated carbon [72-74].

For a given pore size, the adsorptive competition mechanism is controlled by the size of the target compound relative to not only the pore size but also to the size of competing species pore size [71]. In the primary micropore region, because the majority of NOM molecules cannot access it, pore blockage is the dominant mechanism for the reduction in the micropollutant adsorption capacity on activated carbon particles. In the secondary micropore region, the dominant mechanism is through direct competition due to adsorption of a substantial amount of NOM. If the volume of the secondary micropores increase relative to the primary micropores, in other words, usage of heterogeneous micropore size distribution reduce to competitive effect [23]. To prevent pore blockage due to NOM adsorption, an effective adsorbent micropore size distribution should extend to twice widths of the kinetic diameter of target adsorbate [50]. But, there has not been

enough detail study to show pore size effect on adsorption capacity competition mechanism for SPAC vs PAC particles.

High NOM loading causes the pore blockage while low NOM loading leads to the direct competition mechanism [35, 71, 74]. Low MW NOM is highly adsorbed higher MW NOM, which exerts a strong competitive effect on micropollutant adsorption because NOM can access the same adsorption sites with micropollutants [15, 72, 74]. That claim is valid for superfine powdered activated carbon particles in NOM solutions. For example, if the molecular weight of NOM is similar to MIB/geosmin in a natural water, then the competition becomes more severe because NOM and SOCs compete for similar pore sizes [16].

For the SPAC adsorption competition mechanism, it was published that NOM existence in water does not cause the reduction of MIB/geosmin adsorption capacity on SPAC. It was published that MIB is adsorbed internal pores of activated carbon, so enhancing the NOM removal does not induce the less effective removal of MIB [39]. The another explanation is that competing NOM with MIB/geosmin is just 0.2- 2% of entire NOM and it has similar competition impact both SPAC and PAC [49]. Though SPAC has higher NOM adsorption capacity than PAC, the NOM impact on micro-pollutant adsorption capacity is not more severe for SPAC than PAC.

Although adsorption competition mechanism between NOM and SOC are not crystal clear, there are simple quantitative model approaches such as ideal adsorption

solution theory. One of the approaches is the equivalence background compound (EBC) which uses to distinguish between adsorption of NOM and NOM fraction that directly competes with SOCs [39]. Based on that approach, Matsui et al. [39] proposed that SPAC and PAC adsorb same fraction of competing NOM (MW<230 Da) which is the 0.2-2 % of entire NOM even if SPAC adsorb more NOM than PAC. In other words, the large amount of NOM adsorbed on SPAC performed the similar extent of competition to such as geosmin adsorption as the small amount of NOM adsorbed onto PAC, which leads the less severe adsorption competition effect on SPAC than PAC. Moreover, if more NOM molecules can reach the interior region of carbon particles, a greater degree of competition can be seen.

CHAPTER 3

3 RESEARCH OBJECTIVES

The main motivation for this work is to improve our understanding of mechanisms and factors controlling adsorption of four different SOCs on SPAC and compared to their adsorption by PAC adsorption. Specifically, this research project focused on four objectives.

1. ***The first objective was to understand the impact of crushing on carbon characteristics.*** To achieve this goal, the characterization of PAC particles and their crushed SPAC forms by nitrogen adsorption analysis. C/H/N/O and ash content analysis, pH_{PZC} measurement and theoretical calculations were conducted and compared. The characterization results were also used to interpret the SOC adsorption results in aqueous solution.

2. ***The second objective was to investigate the SPAC adsorption capacity and rate for selected SOCs in distilled and deionized water (DDW) and natural waters from Myrtle Beach, South Carolina and compare with PAC adsorption.*** To accomplish this goal, phenanthrene (PNT), atrazine (ATZ), carbamazepine (CMZ) and 2 phenylphenol (2PP) isotherm and kinetics adsorptions were conducted on SPAC and PAC in distilled and deionized water (DDW) and natural waters from South Carolina.

3. ***The third objective was to gain inside adsorption mechanism(s) of the selected SOCs on SPAC and PAC.*** The four SOCs selected for this study have different planarity, polarity, and hydrogen/electron donor/acceptor ability, to allow investigating adsorbate and adsorbent interactions.

CHAPTER 4

4 MATERIALS AND METHODS

4.1 Adsorbents

Coal-based Watercarb (WC) 800 PAC was prepared as slurry stock solutions in DDW and pulverized to super-fine particles with a wet bead mill from Netzsch Premier Technologies LLC.. The adsorbent stock solution had concentration of 200 mg/L and was stored in refrigerator all time.

4.2 Adsorbates

Phenanthrene (PNT, 99.5+%), 2-phenylphenol (2PP, 99+%), and carbamazepine (CMZ,99+%) were obtained from Sigma-Aldrich Chemical Co. Their 1 ppm stock solutions were prepared in methanol. Radiolabelled (carbon-14) atrazine was purchased from American Radiolabelled Chemicals, Inc., and used in conjunction with non-labelled atrazine from AccuStandard. Both labelled and non-labelled atrazine stock solution were prepared in ethanol and stored in separate sealed bottles under refrigerator. The stock solution with an activity of 100 mCi/mmol was prepared with a labelled to non-labelled atrazine ratio of 1:300, due to high specific activity and cost of labelled atrazine. The properties of the four SOCs are summarized in Table 4.1 and their molecular configurations are schematically shown in Figure 4.1.

Table 4.1 Pysicochemical properties of SOCs

	MW[a]	**LogK$_{OW}$**[b]	**S$_W$**[c]	**MV**[d]	**Dipole Moment**[e]	**Molecular Sizes**[f]	**Molecular Configuration**	**Molecular Polarity**
	(g/mol)		(mg/L)	(cm^3/mol)	(Debye)	(Å)		
PNT	178.2	4.68	1.1	157.6	0.34	11.7× 8 × 3.4	Planar	Nonpolar
ATZ	215.6	2.61	34.7	169.8	1.76	9.6× 8.4 × 3	Planar	Polar
CMZ	236.7	2.45	112	186.5	3.64	12×8.9×3.2	Nonplanar	Polar
2PP	170.2	2.94	700	140.3	2.21	11.8× 7.8 × 5.4	Nonplanar	Polar

[a] Molecular weight; [b] Simulated with ACDLABS11.0 (ChemSketch and ACD/3D Viewer); [c] Water solubility at 25^0 C obtained from the Material Safety Data Sheet of each compound; [d] Molecular Volume; [e] and [f] Simulated with ACDLABS11.0 (ChemSketch and ACD/3D Viewer).

PNT

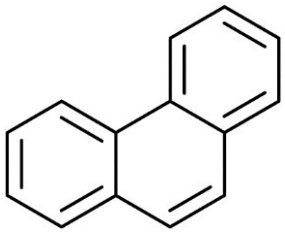

ATZ

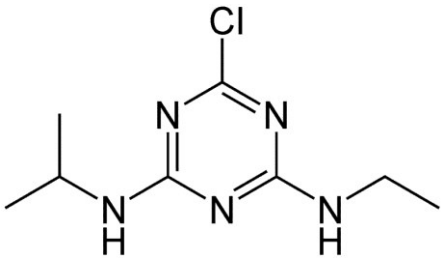

CMZ

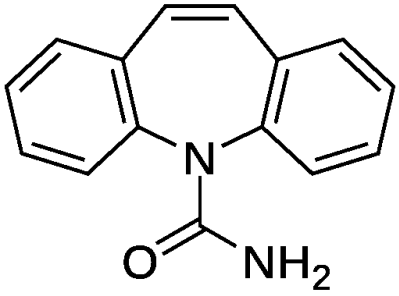

2PP

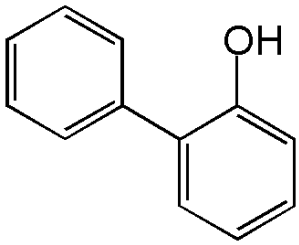

Figure 4.1 Molecular structures of SOCs

4.3 Characterization of Adsorbents

The physicochemical properties of adsorbents were characterized by using various techniques: (i) Nitrogen adsorption for surface area and pore size distribution (PSD) (ASAP 2010 Physisorption/Chemisorption Analyzer,Micromeritics); (ii) elemental analysis for the determination of carbon, hydrogen, nitrogen, and oxygen (CHNSO elemental analyzer); and (iii) the pH of the point of zero charge (pH_{PZC}). In addition, carbon was burned at 600^0C and ash dissolved in 200 mL nitric acid was sent to Agricultural Service Laboratory of Clemson University to analyze ash content. Moreover, the particle size was provided from DLS measurements by milling company. Furthermore, external surface area of the carbon particle was calculated as spherical particles assumption by ignoring space between particles.

4.3.1 Surface Area and Pore Size Distribution

Nitrogen gas adsorption isotherms, volumetrically obtained in the relative pressure range of 10^{-6} to 1 at 77 K on a Micromeritics ASAP 2010 Physisorption Analyzer, was used to determine the surface area and pore size distribution of the samples. Surface area was calculated from Brunauer-Emmett-Teller (BET) equation. The relative pressure range used for the BET calculation was 0.01 to 0.1. Micromeritics Density Functional Theory (DFT) software was used to determine the pore size distribution. A graphite model with slit shape pore geometry was assumed in the pore

size distribution calculation. The adsorbed volume of the nitrogen near saturation point ($P/P_o = 0.99$) was used to determine the total pore volume.

4.3.2 pH_{PZC}

The pH_{pzc} was determined according to the pH equilibration method [65]. DDW was initially boiled to remove dissolved CO_2. The boiled DDW was used to prepare 0.1M NaCl solutions with the pH in the range of pH 2 to pH 11 adjusted with either 0.1N HCl or 0.1N NaOH solutions. In 40 ml vials, 100 mg of activated carbon sample was mixed with 20 ml of the 0.1M NaCl solutions of different pH values in a glove box. The vials were shaken at 200 rpm on a table shaker at room temperature for 24 hours, and then were left on a bench to allow the activated carbons to settle down. The final pH of the solution was measured using a pH meter. The pH_{pzc} was determined as the pH of the NaCl solution which did not change its pH after contacting with the carbon samples.

4.4 Isotherm and Kinetic Experiments

Constant carbon dose aqueous phase isotherm experiments were conducted using DDW and three natural waters. For natural water samples, Edisto raw (diluted to 4 mg DOC/L), Myrtle Beach raw (diluted to 4 and 10 mg DOC/L), and Myrtle Beach treated (diluted to 4 mg DOC/L) waters were used after filtration by 0.2 μm filter paper and stored in refrigerator. Myrtle Beach treated water was collected from the effluent of sedimentation basin after conventional treatment processes at the Myrtle Beach water treatment plant.

Isotherm experiments were performed in 255, 125, 125 and 65 mL glass bottles with Teflon lined screw caps for PNT, CMZ, 2PP, and ATZ, respectively. The carbon dose was 4 mg/L for PNT, 2PP, ATZ and 8 mg/L for CMZ. Concentrated stock solutions of PNT, 2PP and CMZ adsorbate were prepared in methanol, ATZ were prepared in ethanol. The bottles were first filled with water samples to nearly full, and then were spiked with predetermined volumes of stock adsorbate solutions. The head space free bottles were then placed on a tumbler for one week at room temperature (21 ± 3°C). After equilibration, bottles were placed on a bench for one hour without disturbance to allow settling of the adsorbents. Samples were withdrawn from the supernatant and concentrations were analyzed using high performance liquid chromatography (HPLC).

Bottle point kinetic experiments were conducted using the same bottles, carbon doses, and analytical techniques as described for isotherm experiments. The head space free bottles filled by DDW and/or NOM solutions spiked with constant volumes of stock adsorbate solutions. After, bottles were opened each 1.5 hours, 2 hours, 4 hours and 6 hours later. All samples were withdrawn from the supernatant instantaneously and centrifuged at 3500 rpm for 10 min before measuring the final concentration.

A 4.6 x 150 mm and 5-micron size HPLC column (Agilent / Zorbax Extend-C18) was used at a flow rate of 1 mL/min for analyses of PNT and 2PP. PNT was measured by UV detector at 250 nm eluted by 80% methanol and 20% DDW; 2PP was measured by UV detector at 245 nm eluted by 60% methanol and 40% DDW.

A 4.6 x 150 mm reversed phase 5- micron size HPLC column (Supelco / C18) was used at a flow rate of 1 mL/min for analyses of CMZ. CMZ was detected by UV detector at 210 nm eluted by %50 methanol and %50 DDW.

For the detection of ^{14}C-atrazine, 5 mL of sample and 5 mL of liquid scintillation cocktail (UltimateGold XR) were analyzed in liquid scintillation counting (Wallac 1415) during 15 minutes.

4.5 Isotherm modeling

Three isotherm models, Freundlich, Langmuir, and Polanyi-Manes models, were applied to the experimental data.

The Freundlich model is an empirical equation, and it is widely used nonlinear sorption model owing to describe much adsorption data for heterogeneous adsorbent surfaces. This model is expressed as:

$$q_e = K_F C_e^{\,n} \qquad (4.2)$$

Where, q_e is the solid-phase equilibrium concentration (mg/g); C_e is the aqueous phase equilibrium concentration (µg/L or mg/L); K_F is the Freundlich equilibrium affinity parameter ((mg/g)/C_e^n), n represents the exponential parameter related to the magnitude of the driving force for the adsorption and the distribution of adsorption site energies, and it ranges between 0 and 1 [75]. A larger K_F value represents a larger adsorption affinity,

whereas a larger *n* value indicates a more homogeneous surface of the adsorbent [66, 76, 77].

The Langmuir model has a theoretical basis, and it is generally the most straightforward non-linear isotherm model on monolayer adsorption. The Langmuir equation is:

$$q_e = \frac{q_m b C_e}{1 + \mathrm{bC_e}} \tag{4.3}$$

Manes and co-workers [78, 79] developed the Polanyi adsorption potential theory. Later, the theory was referred as the Polanyi-Manes model which is widely used for adsorption surfaces with heterogeneous energy distribution:

$$q_e = q_m \times 10^{[\alpha\left(\frac{\varepsilon}{V_s}\right)^b]} \tag{4.5}$$

Where, *a* and *b* are fitting parameters; *V*s is molar volume of solute; ϵ is the Polanyi adsorption potential expressed as $\epsilon = RT \ln(C_s / C_e)$ [kJ/mol]; C_s is the water solubility of the adsorbate; *R* is the ideal gas constant and *T* is the absolute temperature.

CHAPTER 5

5 RESULT AND DISCUSSION

5.1 Characterization of Adsorbents

Physical characteristics such as particle mean diameter (D), specific surface area (S_{BET}), total pore volume (V_T) and pore size distribution are shown in Table 5.1. After grinding PAC into SPAC, particle mean diameter decreased from 21 to 0.42 microns. The BET surface area measurements showed that the total surface area of SPAC was lower than its precursor PAC, even though SPAC had a smaller particle size and higher external surface area (S_{ext}) than PAC. Furthermore, the measured total pore volume was higher for SPAC than PAC, while SPAC had lower micropore volume but higher mesopore volume as compared to PAC. The results suggest that crushing resulted in the collapse of some micropores and a decrease in surface area, while the increased in mesopore and total pore volumes could be due to enlargement of some pores towards the outer region of PAC and/or high degree of aggregation of SPAC particles resulting in the formation of interstices spaces between the pores contributing to the total pore volume determination. These observations were consistent with those reported by Ellerie et al. [42] for one SPAC and its PAC. However, the effect of crushing on the characteristics of PAC in literature is not consistent. Matsui and co-workers reported in general that there was no significant difference in the surface area and pore size distribution of SPACs and an their PAC forms [10, 16, 36, 45, 74]. On the other hand, Dunn et al. [32] reported similar

surface areas and micropore volumes for five SPACs and their PAC forms, while significantly higher mesopore volumes were observed for SPACs than PACs except one. The variability observed in the literature is likely due to the differences in the characteristics of carbons, their raw materials and crushing techniques and procedures used. Currently, additional work is being conducted in our research group to better understand the effect of crushing of different activated carbons.

Table 5.1 Surface Area, Pore size and Particle Size of Adsorbents*

	S_{BET}[a]	S_{ext}	V_T[b]	Pore Volume Distribution[c]			Pore Surface Area[d]			D_p[e]
	(m^2/g)	(m^2/g)	(cm^3/g)	(cm^3/g)			(cm^2/g)			(μm)
				Micropore (<2 nm)	Mesopore (2 - 50 nm)	Macropore (>50 nm)	Micropore (<2 nm)	Mesopore (2 - 50 nm)	Macropore (>50 nm)	
PAC	713	0.63	0.49	0.23	0.15	0.11	522	70	1	21
SPAC	542	32	0.80	0.14	0.18	0.48	309	30	93	0.42

[a]Specific surface area calculated with the Brunauer-Emmett-Teller (BET) model; [b]Total pore volume calculated from single point adsorption at P/P_0 = 0.99; [c,d]The pore volume distribution and surface area in each pore size range obtained from the density functional theory (DFT) analysis; [d]Mean particle size diameter.* Reported results were average of duplicate measurements.

The chemical composition, ash content and pH_{pzc} of carbons were summarized in Table 5.2. SPAC had nearly three times higher nitrogen and four times higher oxygen content than PAC. During grinding process, DDW was used with DARVAN 821A which is ammonium polyacrylate solution, which might be the reason of rise of nitrogen content of carbon particles. Also, the notable increase in the oxygen content and a decrease in the pH_{pzc} of the activated carbon particles from 10.3 to 8.9 were observed as a result of crushing, which caused the decrease in positive charge on carbon surface. Both carbons were still basic in nature. In addition, SPAC had more ash content than PAC (Table 5.2). The elemental analysis of the ash content showed a significant increase, from 0.4% to 15% in the iron content of the (Table A1). The mill used for crushing was made of steel, which is the alloy of essentially iron and carbon elements, which is likely to source of the observed increased iron content [80]. Therefore, one possibility of the increased oxygen content may be related to the oxygen bound with iron rather than carbon surface. Unfortunately, the impact of crushing on the chemical characteristics of activated carbons has not been reported. The current work in our laboratory also examines the effect of crushing of the chemical characteristics of different activated carbons.

Table 5.2 Chemical Characteristics of Adsorbents*

	Elemental Analysis %				Ash %	pH_{PZC}
	C	H	N	O		
PAC	72	0.01	3.1	2.9	22	10.3
SPAC	46	0.7	8.3	10.6	34	8.9

* Reported results were average of duplicate measurements.

5.2 Phenanthrene Adsorption

5.2.1 Phenanthrene (PNT) Isotherms

The single solute PNT adsorption isotherms in DDW for SPAC and PAC are shown in Figure 5.1. In DDW, PNT adsorption isotherm on SPAC and PAC differed from each other. PAC had higher adsorption capacity than SPAC at lower concentrations but at higher concentrations there was no notable difference. This difference can also be seen from the Freundlich capacity K_F^U (in µg/L), and K_F^M (in mg/L) values tabulated in Table 5.3. The K_F^U (in µg/L) representing the lower concentration ranges were ~10 times higher for PAC than SPAC; whereas, K_F^M (in mg/L) representing higher concentrations were almost identical. This was attributed to the micropore filling mechanism. The molecular dimensions of the PNT ($11.7 \times 8 \times 3.4$ Å) are comparable to the micropore dimensions (< 20 Å). Therefore, micropores play a dominant role in the adsorption due to higher adsorption energies resulting from multiple contact points between the adsorbate

molecules and micropores. Calculations have shown that the adsorbed PNT molecules would occupy up to 0.15 cm3/g in the activated carbon pores. Since PAC (micropore volume=0.23 cm3/g) was more microporous than SPAC (micropore volume=0.14 cm3/g), it was more favorable for PNT adsorption than SPAC. In addition, due to more oxygen content of SPAC and PAC, the water cluster formation around the surface oxygen functionalities may hinder adsorption of PNT molecules on SPAC than PAC. Also, surface area (S_{BET}) normalization was also performed but isotherms did not converge notably as seen in Figure A.1. This indicates that SPAC surface area alone was not the controlling factor the adsorption. However, micropore volume normalization was performed for PNT in DDW in Figure 5.2. As seen from figure, data points were converged especially for higher concentration, which supported the micropore filling mechanism.

Also as illustrated in Figure 5.1, PAC performed better than SPAC under NOM competition that was spiked simultaneously with PNT. The presence of NOM resulted in a reduction in PNT adsorption on both adsorbents with increasing concentration as represented by the K_F^M (in mg/L) values, and a decrease in isotherm slope represented by the n values tabulated in Table 5.3. These reductions were attributed to the competition of NOM with PNT molecules for available sorption sites and increasing heterogeneity of sorption sites under NOM loading.

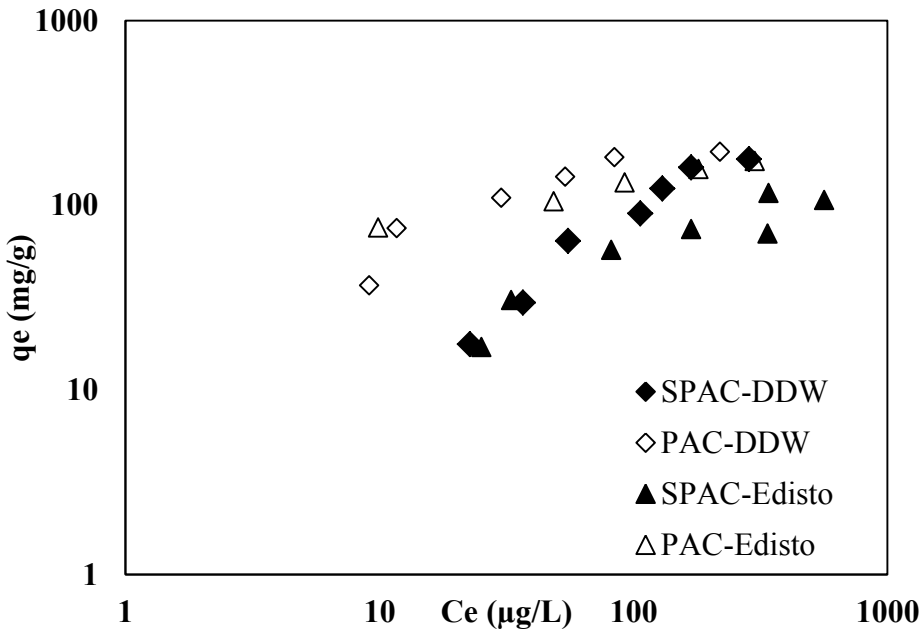

Figure 5.1 PNT adsorption isotherms for SPAC and PAC in DDW and Edisto River raw water with 4 mg DOC/L

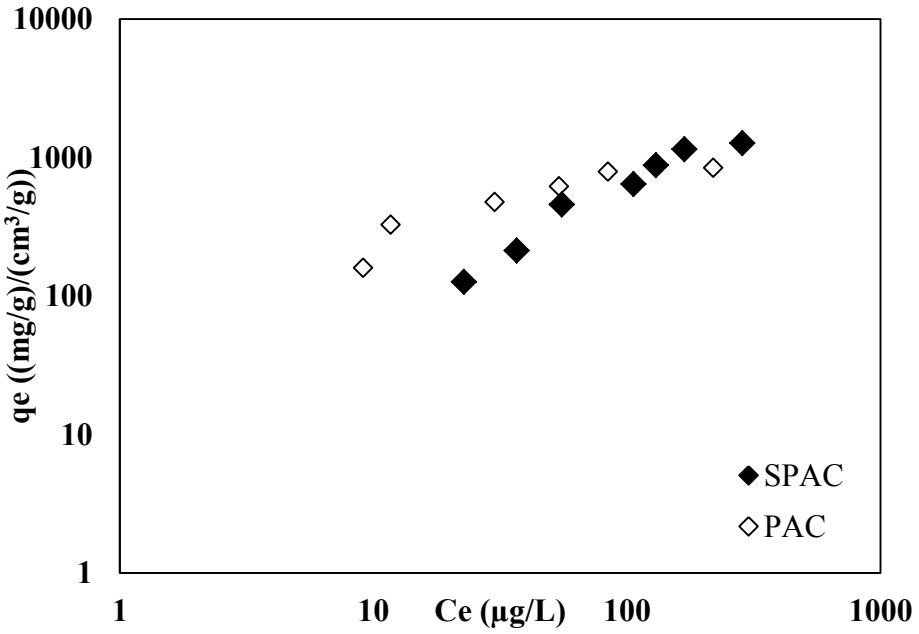

Figure 5.2 Micropore Volume Normalization of PNT adsorption isotherms for SPAC and PAC in DDW.

The adsorption of PNT on SPAC and PAC under different DOC concentrations (4 and 10 mg DOC/L) is shown in Figure 5.3. Higher DOC concentration caused more competition, thus decreased the PNT adsorption. *n* values did not change much, while the value of K_F decreased with increasing DOC concentration((see K_F^M (mg/L) values in Table 5.3 [77]). Thus, increasing DOC concentration did not change the energy distribution of the adsorption sites; even though, the availability of adsorption sites to the target SOC molecules were decreased. This suggests some pore blockage that resulted in the parallel shift of the Freundlich isotherms.

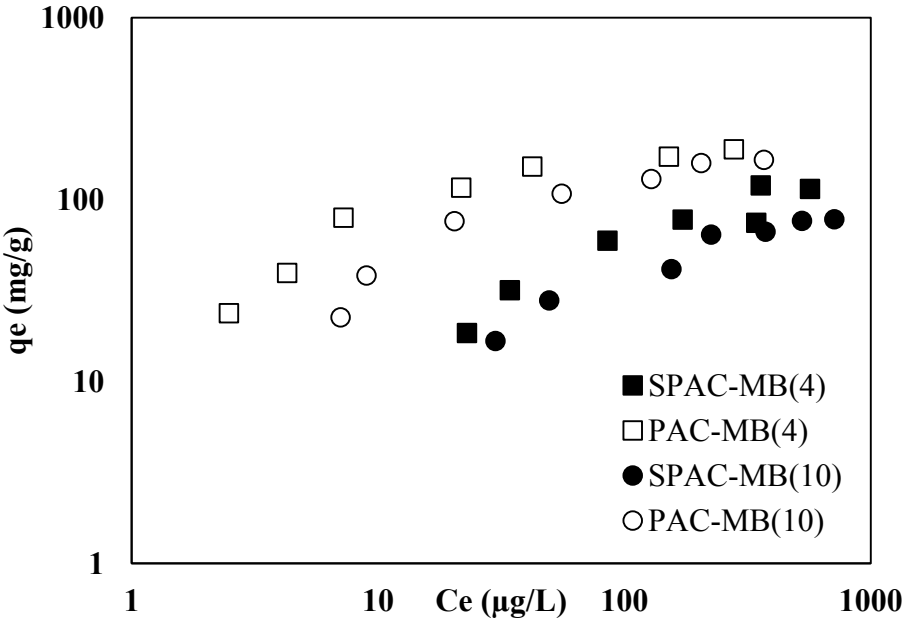

Figure 5.3 PNT adsorption isotherms in MB raw waters with 4 mg DOC/L and 10 mg DOC/L

PNT adsorption on SPAC and PAC in raw and treated (i.e., after conventional treatment processes) was compared in Figure 5.4. Raw water DOC level was adjusted to

that of treated water with dilution but the waters had different $SUVA_{254}$ (UV_{254}/DOC) values. The raw water had a higher $SUVA_{254}$ (4.4 L/mg.m) value indicating the presence of higher molecular weight and more aromatic components than the raw water with low $SUVA_{254}$ (2.1 L/mg.m) values. PNT was not drastically influenced by the changing nature of NOM. This suggests that adsorption of PNT molecules, because of small molecular dimension and highly hydrophobic nature, was not greatly impacted with changing composition of background NOM characteristics..

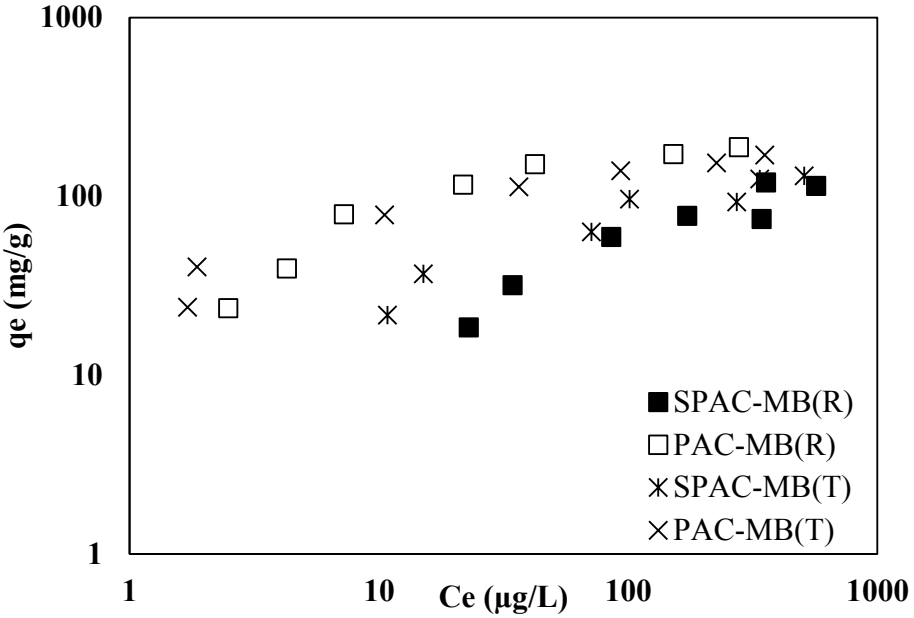

Figure 5.4 PNT adsorption isotherms in MB raw and treated waters with 4 mg DOC/L

All isotherms modeling results were listed in Table 5.3. They were nonlinear when the q_e vs C_e values were plotted on linear coordinates. Therefore, three widely used nonlinear isotherm models, Freundlich (FM), Langmuir (LM), and Polanyi-Manes models (PMM), were employed to fit the experimental data with Microsoft Office Excel

2007 (Table 5.3). Coefficient of determination (r^2) were used to evaluate the goodness of fit. Generally, the FM provided better fit to adsorption on SPAC experimental data than the two-parameter LM and PMM (Table 5.3). The PMM and LM had higher r^2 values for most of the isotherms of PAC than the FM

Table 5.3 Nonlinear model fits of adsorption of PNT on SPAC and PAC

	ISOTHERMS	Freundlich				Langmuir				Polanyi-Manes		
		K_F^U μg/L	K_F^M mg/L	n	r^2	q_m	K_L	r^2	q_m	a	b	r^2
SPAC	DDW	1.1	764	0.85	0.952	380	0.003	0.957	209	-4764	2.84	0.888
	Edisto Raw=4mg DOC/L	4.2	167	0.53	0.871	126	0.009	0.859	114	-464	2.17	0.834
	MB Raw=4mg DOC/L	4.5	172	0.53	0.907	134	0.008	0.883	132	-91.2	1.91	0.839
	MB Raw=10mgDOC/L	3.8	105	0.48	0.847	194	0.001	0.702	78	-353	2.07	0.972
	MB Treated=4mg DOC/L	9.9	190	0.43	0.923	137	0.017	0.922	134	-165	1.96	0.934
PAC	DDW	18.1	512	0.48	0.839	237	0.028	0.958	200	-11243	3.53	0.97
	Edisto Raw=4mg DOC/L	72.6	140	0.09	0.715	170	0.056	0.929	219	-24.1	1.35	0.971
	MB Raw=4mg DOC/L	24.7	416	0.41	0.845	194	0.074	0.988	198	-823	2.74	0.965
	MB Raw=10mgDOC/L	13.4	328	0.46	0.893	178	0.029	0.983	168	-985	2.63	0.996
	MB Treated=4mg DOC/L	28.8	277	0.33	0.916	162	0.09	0.967	171	-109	2.07	0.977

K_F (L/μg): Freundlich adsorption affinity coefficient; n: nonlinear index; r^2: coefficient of determination; q_m (mg/g): maximum adsorption capacity; K_L (L/μg): Langmuir adsorption affinity coefficient; a and b: fitting parameters; underlined numbers represent the unreasonable values of PMM modeling.

5.2.2 Phenanthrene Adsorption Kinetics

The adsorption kinetics of PNT was investigated in both DDW experiments and in the presence of background NOM of 4 mg DOC/L for raw (Edisto River and Myrtle Beach) and treated (MB) water and 10 mg DOC/L for raw MB water. Adsorption kinetics results clearly showed the PNT uptake rate was faster by SPAC than PAC in all solutions (Figure 5.5 to 5.7), which was consistent with the geosmin and MIB adsorption kinetics in literature [16].

PNT adsorption kinetics in DDW and NOM solution are shown in Figure 5.5. In DDW, about 90% PNT removal was attained within just 2 hours, while PNT removal with PAC was up to 70% at the same point. This was attributed to the higher external surface area of SPAC due to its smaller size (Table 5.1). Moreover, after crushing SPAC had higher macropore volume than PAC, which seems to provide a kinetic advantage for the target PNT molecule to access the pore network. Thus, lower PNT residual concentration in aqueous phase was obtained in the first 6 hours even though PNT molecules may or may not have reached its target adsorption sites. The data indicates that adsorption rate slowed down after 6 hours contact time. On the other hand, the adsorption capacity of PAC was higher than SPAC for PNT adsorption; although SPAC showed faster adsorption kinetics than PAC. This was due to higher surface area and microproposity of PAC.

In the presence of 4 mg DOC/L background NOM (raw Edisto) solution, PNT uptake rate was slightly decreased with respect to the rate in DDW for both activated carbons (Figure 5.4). SPAC still showed faster and higher degree of PNT removal than PAC.

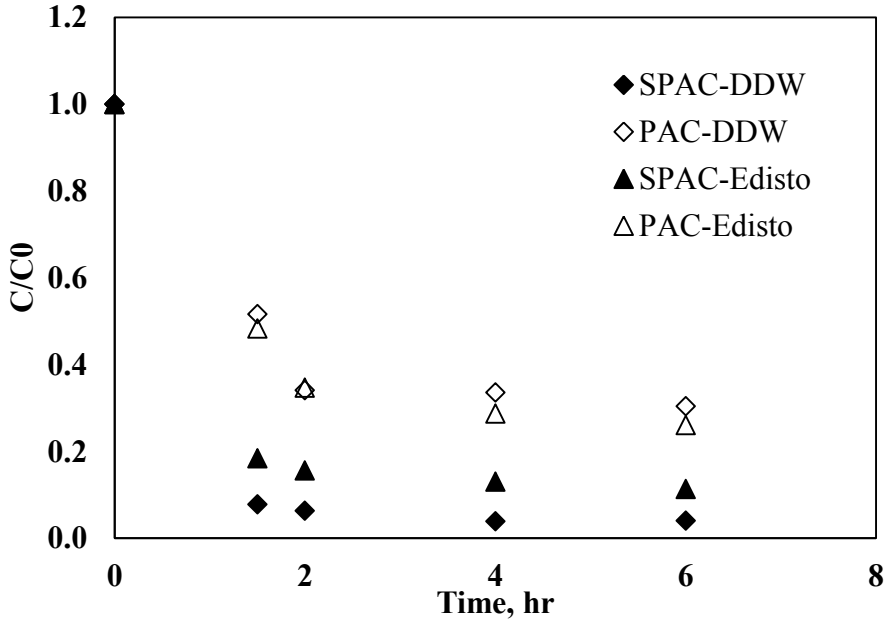

Figure 5.5 PNT adsorption kinetics for SPAC and PAC in DDW and Edisto River raw water with 4 mg DOC/L.

Figure 5.5 shows the effect of NOM concentration on PNT adsorption kinetics SPAC and PAC. Doubling NOM concentrations resulted in a small impact on PNT adsorption. Since PNT is a small molecular weight hydrophobic compound that can adsorb faster and also having higher affinity to carbon surface, the presence of NOM molecules did not make a significant impact on the adsorption of PNT by PAC and SPAC. Likewise, the comparison of the impact of raw water vs. treated water NOM

(Figure 5.6) did not exhibit a major impact of PNT adsorption. This is probably due to higher adsorption of affinity of PNT to activated carbon surfaces.

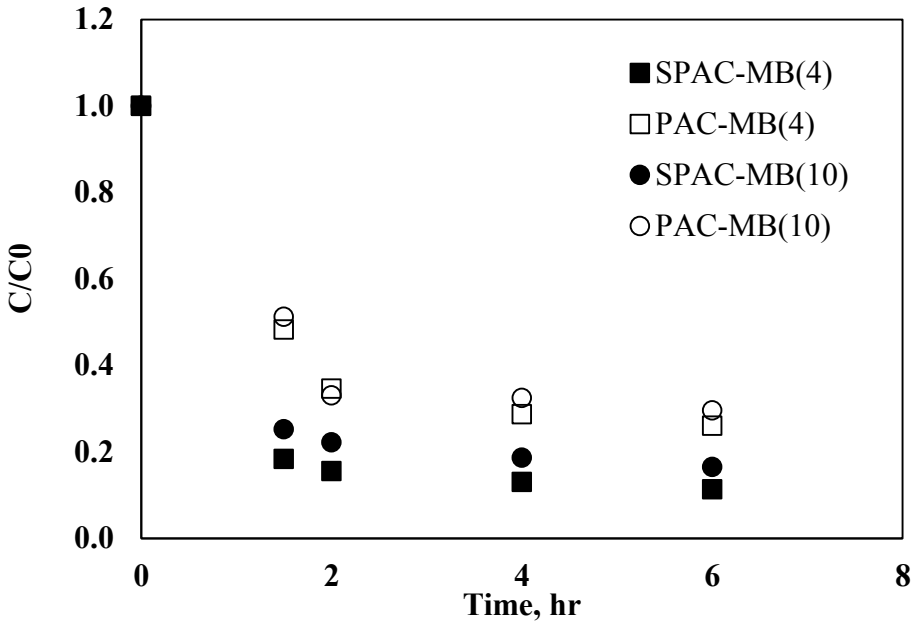

Figure 5.6 PNT adsorption kinetics in MB raw waters with 4 mg DOC/L and 10 mg DOC/L.

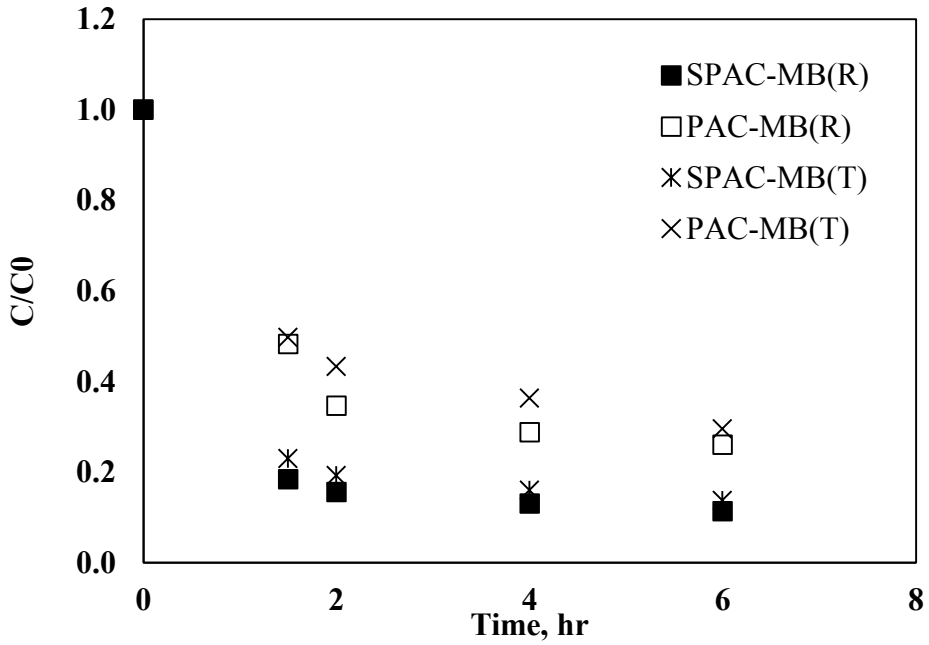

Figure 5.7 PNT adsorption kinetics in MB raw and treated waters with 4 mg DOC/L

5.3 Atrazine Adsorption

The second SOC investigated in this study was atrazine (ATZ) with a similar experimental matrix as conducted for PNT.

5.3.1 Atrazine Adsorption Isotherm

ATZ isotherms on SPAC and PAC in DDW and Edisto water are shown in Figure 5.8. SPAC exhibited lower capacity than PAC in both DDW and Edisto water.

In literature, it was suggested that the 8 to 20Å pore size range is the ideal region for the adsorption [81]. Therefore, PAC having higher amount of micropores with size approaching the dimensions of the ATZ molecules showed higher adsorption capacity

than SPAC, due to higher adsorption energies resulting from multiple contact points between the PAC and ATZ molecules..

Despite some scatter in the data, it was clear from Figure 5.8 that the presence of NOM resulted in much more severe reduction in capacity of PAC than SPAC, which means that pore blockage impact on PAC was more severe than SPAC having mainly macrospores.

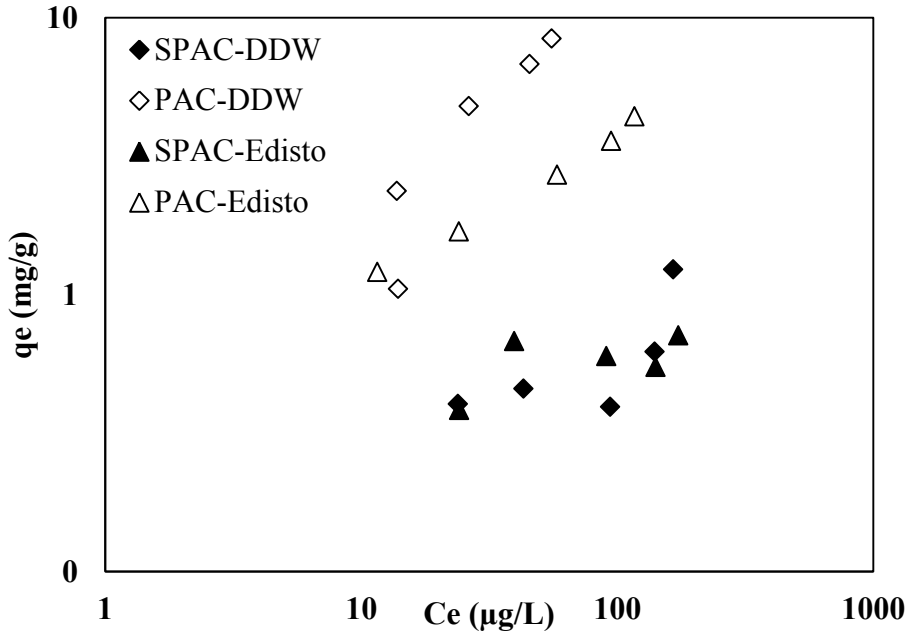

Figure 5.8 ATZ adsorption isotherms for SPAC and PAC in DDW and Edisto River raw water with 4 mg DOC/L

The effect of NOM was also investigated using two different NOM source waters (Edisto and Myrtle Beach) at the same DOC value of 4 mg /L in Figure A.5. The results

did not show significant difference in terms of PAC and SPAC ATZ capacity indicating that the difference in the NOM characteristics ($SUVA_{254}$~ 2 L/mg.m)

4 and 10 mg DOC/L background solution for adsorption on SPAC and PAC displayed in Figure 5.9. Higher NOM concentration increased the competition between ATZ and NOM molecules as seen. Even if ATZ adsorption on SPAC was not affected by the concentration of DOC, concentration of DOC had little influence on ATZ adsorption capacity on PAC. It was claimed that NOM molecules preferentially adsorbed near the outer surface of the SPAC particles and not completely penetrate the adsorbent particle [10]. Only small fraction of NOM can diffuse inner pores of SPAC and compete with SOC [35]. Therefore, competition between ATZ molecules and NOM compounds on SPAC was less severe than on PAC.

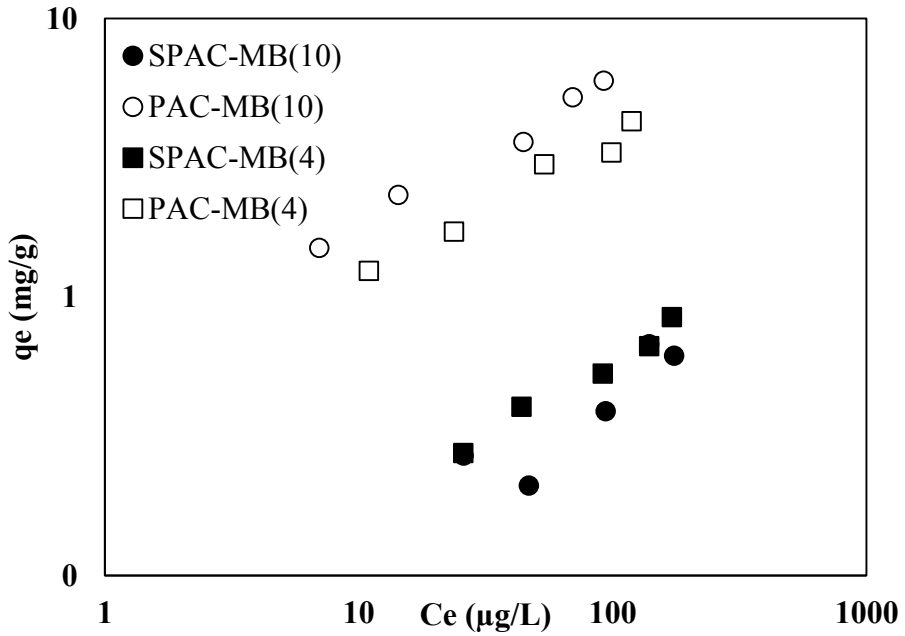

Figure 5.9 ATZ adsorption isotherms in MB raw waters with 4 mg DOC/L and 10 mg DOC/L

High MW of NOM (Raw MB water) and low MW of NOM (Treated MB water) were compared in Figure 5.10. NOM molecular weight did not alter the ATZ adsorption capacity on SPAC. However, PAC highly microporus and larger BET surface area was affected by high MW of NOM, which may arise owing to clogging of pores and ATZ molecules cannot reach inner side of the pores.

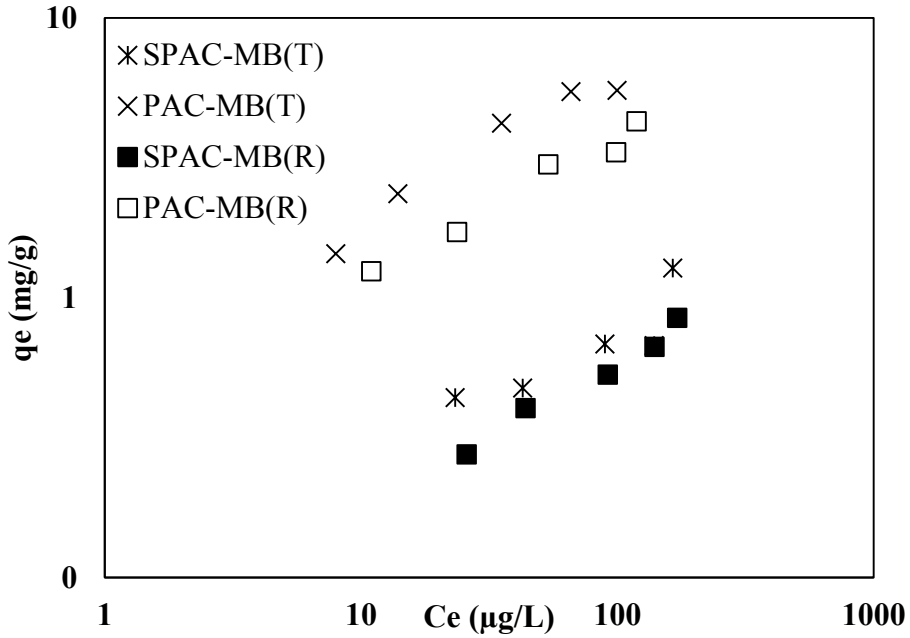

Figure 5.10 ATZ adsorption isotherms in MB raw and treated waters with 4 mg DOC/L.

Because PNT was more hydrophobic than ATZ, ATZ adsorption capacity was lower than PNT adsorption capacity on both SPAC and PAC in all background solutions

Moreover, the isotherms and the corresponding FM, LM and PMM were shown in Table 5.4. Experimental complications led to lower r^2 owing to scattering data points.

Table 5.4 Nonlinear model fits of adsorption of ATZ on SPAC and PAC

	ISOTHERMS	Freundlich				Langmuir			Polanyi-Manes			
		K_F^U μg/L	K_F^M mg/L	n	r^2	q_m	K_L	r^2	q_m	a	b	r^2
	DDW	0.09	2.08	0.46	0.720	1.6	0.01	0.628	681	-9.8	0.46	0.510
	Edisto Raw=4mg DOC/L	0.16	1.1	0.27	0.851	0.7	0.087	0.402	0.61	-1977	4.66	0.890
SPAC	MB Raw= 4mg DOC/L	0.05	2.36	0.54	0.978	1.3	0.009	0.94	33	-9.1	0.64	0.960
	MB Raw=10mgDOC/L	0.06	1.43	0.47	0.867	1.3	0.005	0.825	804	-9.6	0.42	0.963
	MB Treated=4mg DOC/L	0.07	2.91	0.54	0.892	2.8	0.005	0.887	1552	-8.9	0.38	0.630
	DDW	0.24	110	0.88	0.927	194	0.001	0.950	9.9	-6E+08	9.3	0.940
	Edisto Raw=4mg DOC/L	0.30	13.4	0.55	0.992	6.8	0.013	0.96	71.1	-20.54	1.1	0.950
PAC	MB Raw=4mg DOC/L	0.37	11.1	0.50	0.973	5.5	0.021	0.942	6.35	-3526	3.83	0.910
	MB Raw=10mgDOC/L	0.55	20.2	0.52	0.988	8.5	0.022	0.953	215	-18.2	0.96	0.979
	MB Treated=4mg DOC/L	0.52	22.4	0.54	0.951	7.4	0.034	0.985	10.1	-795	3.17	0.970

K_F (L/μg): Freundlich adsorption affinity coefficient; n: nonlinear index; r^2: coefficient of determination; q_m (mg/g): maximum adsorption capacity; K_L (L/μg): Langmuir adsorption affinity coefficient; a and b: fitting parameters; underlined numbers represent the unreasonable values of PMM modeling.

5.3.2 Atrazine Adsorption Kinetics

Atrazine adsorption kinetics was investigated on SPAC and PAC in DDW and natural Edisto waters (4mg DOC/L) showed in Figure 5.11. In DDW, about 95% PNT removal was attained within just 2 hours, while ATZ removal with PAC was up to 80% at the same point like PNT isotherm. SPAC with a larger mesopore volume and higher external surface areas possessed faster sorption kinetics than PAC in both background solutions, especially in DDW. Additionally, PAC was more severely affected by NOM solution than SPAC due to pore blockage.

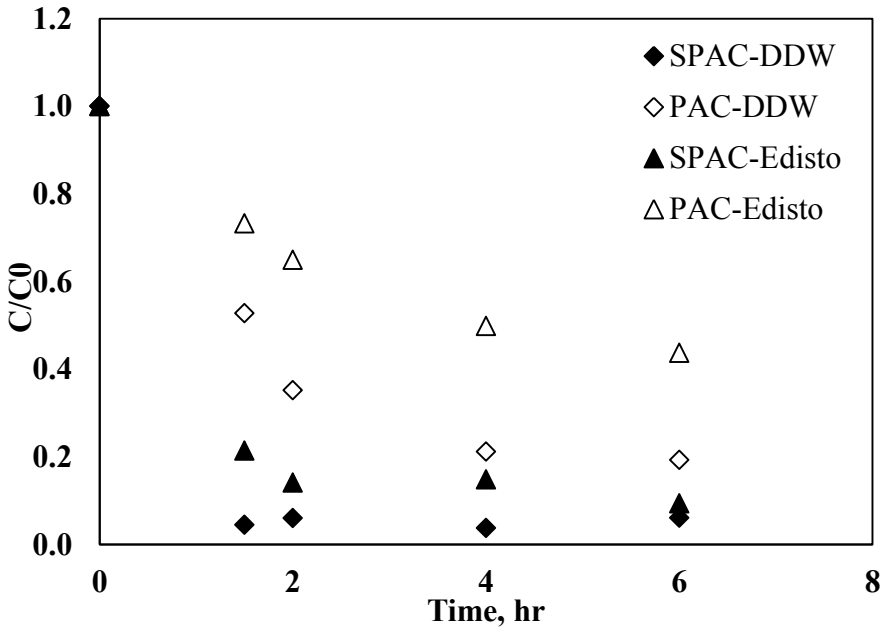

Figure 5.11 ATZ adsorption kinetics for SPAC and PAC in DDW and Edisto River raw water with 4 mg DOC/L

The ATZ kinetics in the presence of different concentration and MW of NOM solutions represented in Figure 5.12 and 5.13, respectively. Also, the NOM type effect showed in Figure A.6 were presented that NOM type did not changed the ATZ kinetics behavior on SPAC and PAC like PNT kinetics.

Figure 5.12 showed the NOM concentration impact on ATZ uptake rate. The presence of background NOM had severe adverse impact on adsorption kinetics of microporous PAC, because more pore blockage competition can be seen on PAC. Especially, concentrated NOM solution (DOC is 10 mg/L) caused more intense competition on PAC particles than dilute NOM solutions. As mentioned before, NOM compound adsorbed mainly exterior region which triggers the pore blockage competition. Because SPAC had higher external surface are, more available external pore spaces lessened the competition effect.

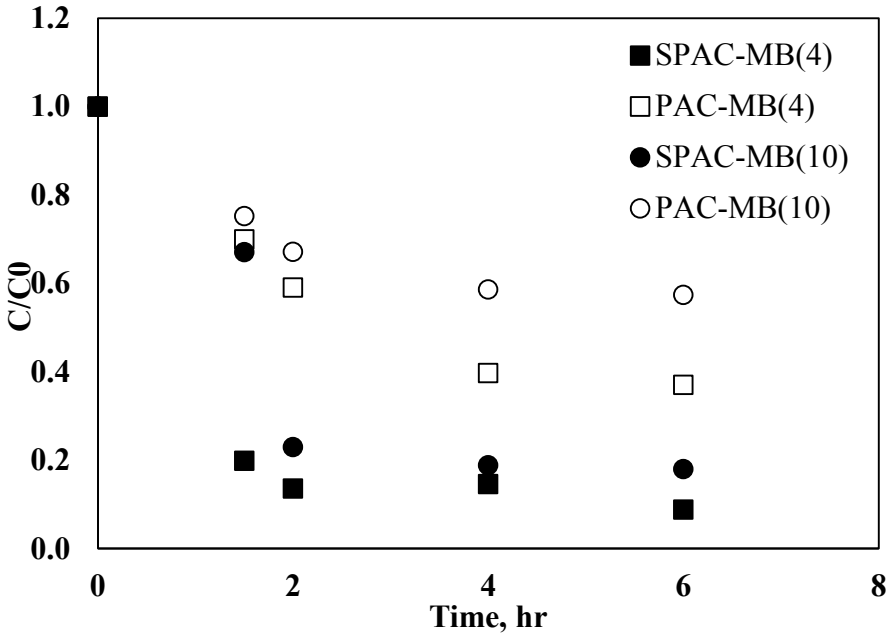

Figure 5.12 ATZ adsorption kinetics in MB raw waters with 4 mg DOC/L and 10 mg DOC/L.

Figure 5.13 investigated the ATZ uptake rate in terms of the NOM compound characteristics. Low MW of NOM induced more competition than high MW of NOM on PAC particles. PAC had higher micropore region and low MW of NOM can compete in greater extent to ATZ particles due to similar particle size.

Similarly with PNT adsorption kinetics, it was observed that the kinetic plots for the microporous large particles (PAC) eventually crossed that of the mesoporous small activated carbon particles (SPAC) and the final equilibrium concentrations corresponded to those observed in the equilibrium isotherm experiments because the saturation rate for large particles were lower than for small particles [10].

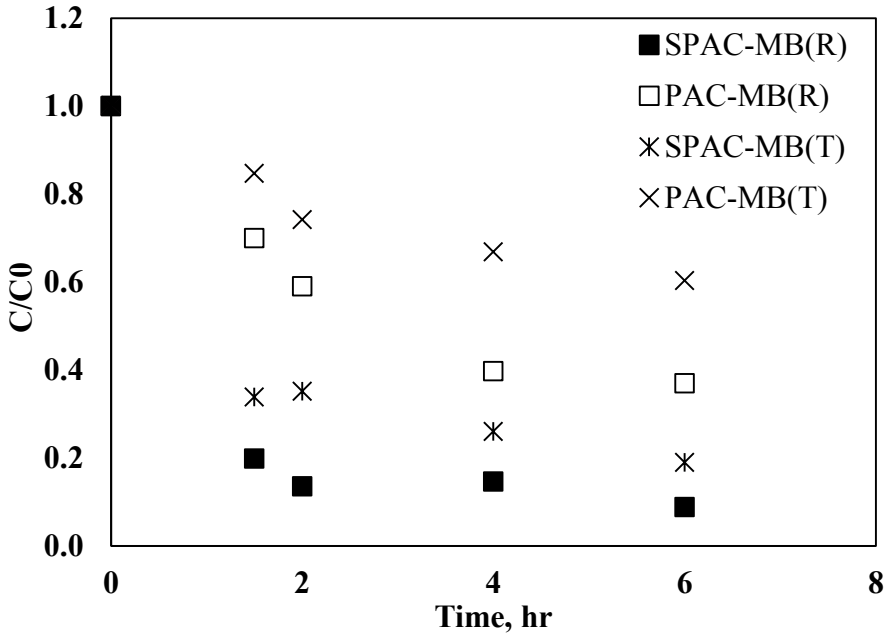

Figure 5.13 ATZ adsorption kinetics in MB raw and treated waters with 4 mg DOC/L

Based on isotherms and kinetics results, NOM more severely affected the ATZ adsorption on PAC than SPAC. However, NOM competition on PNT adsorption on PAC was nearly same with SPAC. The reason might be that more hydrophobic and smaller ATZ molecules can go the deeper pores, and NOM pore blockage effect was more intense on ATZ.

5.4 Carbamazepine Adsorption

As mentioned earlier, the presence of the functional group, molecular conformation, weight, size, polarity and solubility of adsorbate affect adsorption process. To see the adsorbate properties effect on SPAC and PAC adsorption, carbamazepine was chosen due to its molecular size, high solubility, lower hydrophobicity, electron donating

($-NH_2$) and electron withdrawing (C=O) group in its structure (Table 4.1). Therefore, to understand behavior of CMZ adsorption capacity and rate on SPAC and PAC, isotherm and kinetic experiments were done in both DDW and natural waters in different properties.

5.4.1 Carbamazepine Adsorption Capacity

CMZ adsorption capacity on SPAC and PAC in DDW and Edisto river water (4mg DOC/L) were illustrated in Figure 5.14. PAC adsorption capacity of CMZ was slightly higher than SPAC not only in DDW but also in natural waters. Also, the degree of CMZ adsorption capacity reduction owing to NOM competition was similar between SPAC and PAC. Moreover, CMZ adsorption capacity in NOM solution did not differ with respect to water sources, which was seen in Figure A.7.

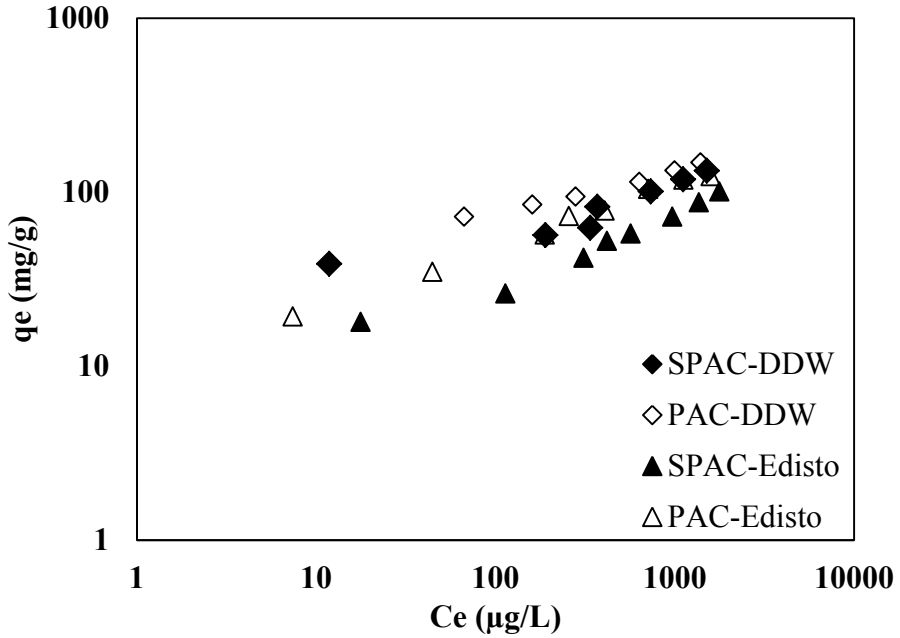

Figure 5.14 CMZ adsorption isotherms for SPAC and PAC in DDW and Edisto River raw water with 4 mg DOC/L

CMZ adsorption behaviors on NOM solution at different conditions were represented in Figure 5.15 and 5.16. They indicated NOM concentration (Figure 5.15) and MW range (Figure 5.16) did not alter the trend of isotherms as understood from $K_F^{U\&M}$ values in Table 5.5, which means CMZ competition with NOM did not depend on concentration and MW of NOM.

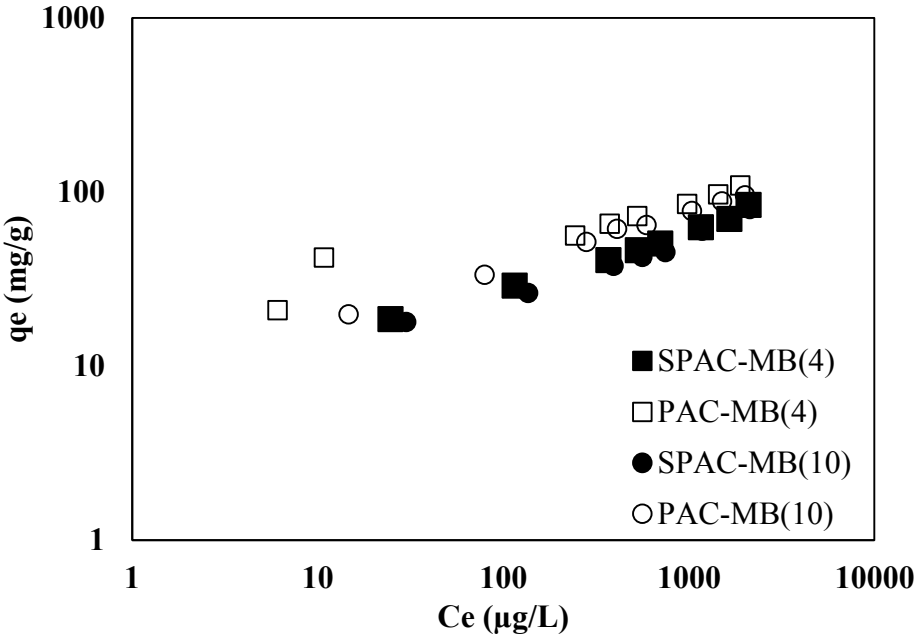

Figure 5.15 CMZ adsorption isotherms for SPAC and PAC in MB raw waters with 4 mg DOC/L and 10 mg DOC/L

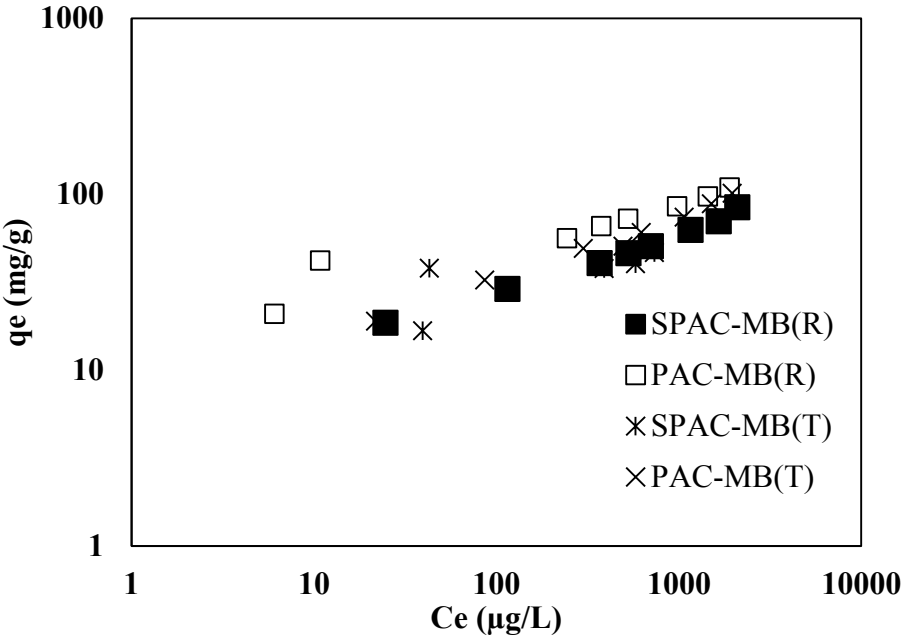

Figure 5.16 CMZ adsorption isotherms in MB raw and treated waters with 4 mg DOC/L

Table 5.5 Nonlinear model fits of adsorption of CMZ on SPAC and PAC

	ISOTHERMS	Freundlich				Langmuir			Polanyi-Manes			
		K_F^U μg/L	K_F^M mg/L	n	r^2	q_m	K_L	r^2	q_m	a	b	r^2
	DDW	18	105	0.25	0.874	162	0.002	0.834	9562	-5.2	0.34	0.901
	Edisto Raw=4mg DOC/L	5.1	73	0.38	0.966	128.6	0.002	0.943	25835	-7.2	0.36	0.944
SPAC	MB Raw= 4mg DOC/L	6.1	60	0.33	0.988	91	0.002	0.869	603	-9.3	0.78	0.938
	MB Raw=10mgDOC/L	5.0	55	0.35	0.976	94	0.002	0.882	41532	-5.1	0.19	0.801
	MB Treated=4mg DOC/L	8.4	56	0.28	0.729	97	0.002	0.59	2203	-4.8	0.38	0.744
	DDW	26	132	0.24	0.985	144	0.01	0.8	4825	-4.0	0.33	0.951
	Edisto Raw=4mg DOC/L	9.2	110	0.36	0.994	139.5	0.004	0.649	250.7	-36	1.6	0.966
PAC	MB Raw=4mg DOC/L	10.4	87	0.23	0.905	84	0.06	0.702	2246	-4.5	0.40	0.94
	MB Raw=10mgDOC/L	8.3	77	0.32	0.998	99	0.004	0.922	297	-12	1.05	0.966
	MB Treated=4mg DOC/L	6.3	74	0.36	0.987	113	0.002	0.883	2927	-6.8	0.51	0.965

K_F (L/μg): Freundlich adsorption affinity coefficient; n: nonlinear index; r^2: coefficient of determination; q_m (mg/g): maximum adsorption capacity; K_L (L/μg): Langmuir adsorption affinity coefficient; a and b: fitting parameters; underlined numbers represent the unreasonable values of PMM modeling.

5.4.2 Carbamazepine Adsorption Kinetics

CMZ adsorption kinetics on SPAC and PAC in DDW and NOM solutions were shown in Figure 5.17 to 5.19. Similar to uptake rates of PNT and ATZ also geosmin and MIB in literature [44], CMZ adsorption kinetics on SPAC were slightly higher than PAC in all background solutions.

Figure 5.17 illustrated the CMZ uptake rate in DDW and natural water. In DDW, SPAC uptakes rate were faster than PAC. In NOM solutions, SPAC also had an advantage over PAC, but this advantage was not larger than in DDW. SPAC was more severely affected by NOM. As seen, the NOM competition effect on SPAC was greater than PAC. Because CMZ size is also large, it might directly compete with NOM for outer region of SPAC. Another important point was that CMZ uptake rate was slower than PNT and ATZ although CMZ and PNT adsorption capacities were similar extent. Because CMZ is slightly larger molecule and highly soluble than PNT with respect to molecular dimensions (Table 4.1), it has slower diffusion rate. Furthermore, CMZ adsorption kinetics did not change with respect to water source as seen in Figure A.8.

The NOM concentration and MW effect on CMZ adsorption capacity can be found in Figure 5.18 and 5.19. Even though, CMZ uptake rate on SPAC was slightly faster than PAC, NOM concentration and/or MW differences did not have impact on CMZ.

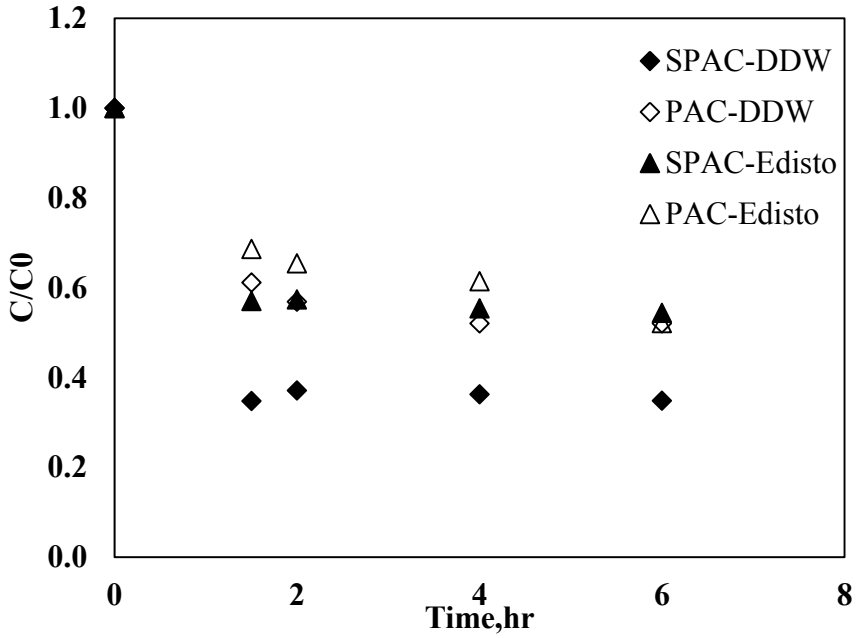

Figure 5.17 CMZ adsorption kinetics for SPAC and PAC in DDW and Edisto River raw water with 4 mg DOC/L

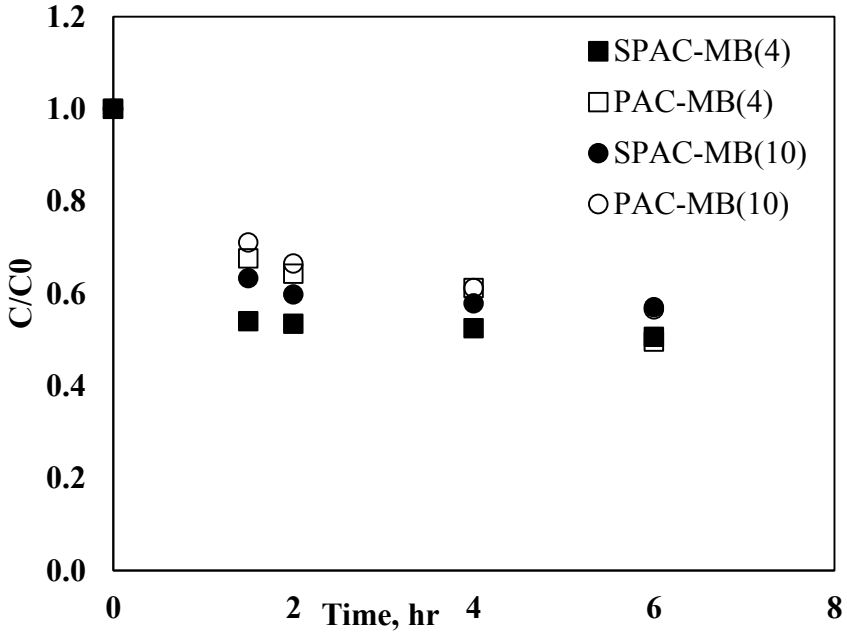

Figure 5.18 CMZ adsorption kinetics in MB raw waters with 4 mg DOC/L and 10 mg DOC/L

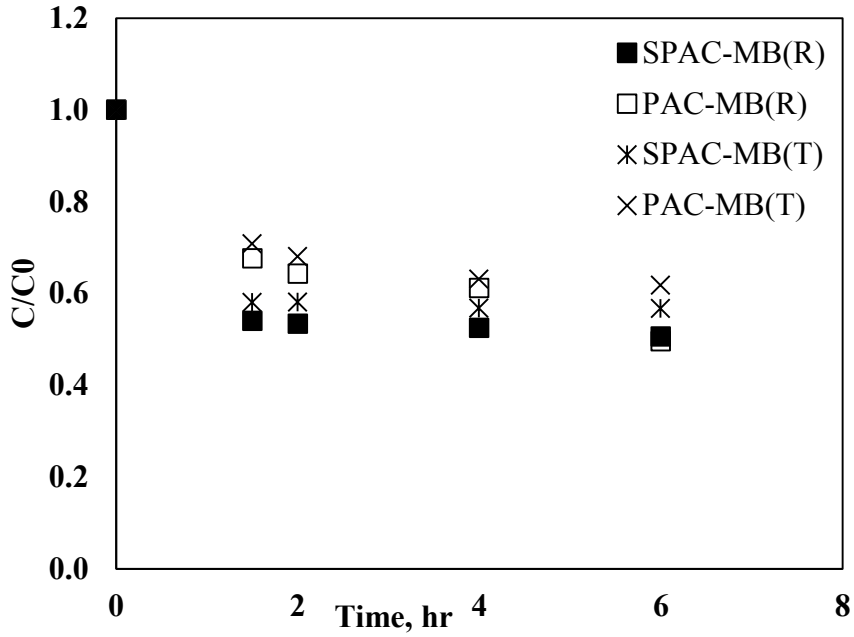

Figure 5.19 CMZ adsorption kinetics in MB raw and treated waters with 4 mg DOC/L

5.5 2-Phenylphenol Adsorption

2PP compound was chosen due to differences in molecular size, hydrophobicity and structure. As distinct from CMZ, 2PP has electron donating hydroxyl group at ortho position. Three possible interaction might be proposed to address these difference: (i) hydrogen bonding between the –OH group on 2PP and oxidized SPAC, or between adsorbed 2PP on carbon surface and dissolved 2PP in solution; (ii) electrostatic interaction; and (iii) π-π EDA interaction between electron poor regions on carbon surface and the electron rich benzene ring of 2PP by electron-donating effect on-OH substitute. To evaluate the 2PP adsorption behavior with respect to time and at equilibrium condition, isotherm and kinetics behavior should be examined.

Crushing process enriched the oxygen content of SPAC surface. Oxidation decreases the dispersive adsorption by reducing π- electron density, but it creates polarity and encourages the adsorption of polar compounds, especially water molecules [53]. On the other hand, 2PP has also polar functional group in its structure, and hydrogen bonding between –OH group on 2PP and SPAC surface might be created. Therefore, SPAC lost its kinetic advantages due to competition adsorption of water molecules and 2PP on oxidized carbon surfaces. Moreover, greater solubility and lower hydrophobicity of 2PP might affect adsorption on SPAC.

5.5.1 2-Phenylphenol Adsorption Isotherm

2PP adsorption capacity in DDW and different NOM solutions was showed in Figure 5.20 to 5.22. As seen in figures, PAC showed greater adsorption capacity than SPAC in all conditions similar to PNT, ATZ and CMZ adsorption isotherms.

Figure 5.20 showed the 2PP adsorption on SPAC and PAC both DDW and NOM solution. In DDW, adsorption capacity of PAC was higher than SPAC even if NOM competed with 2PP and reduced the capacity. Also, it was clearly seen that NOM solution caused the change in slope both PAC and SPAC, which means that NOM may induce the change in surface heterogeneity on SPAC and PAC for 2PP adsorption.

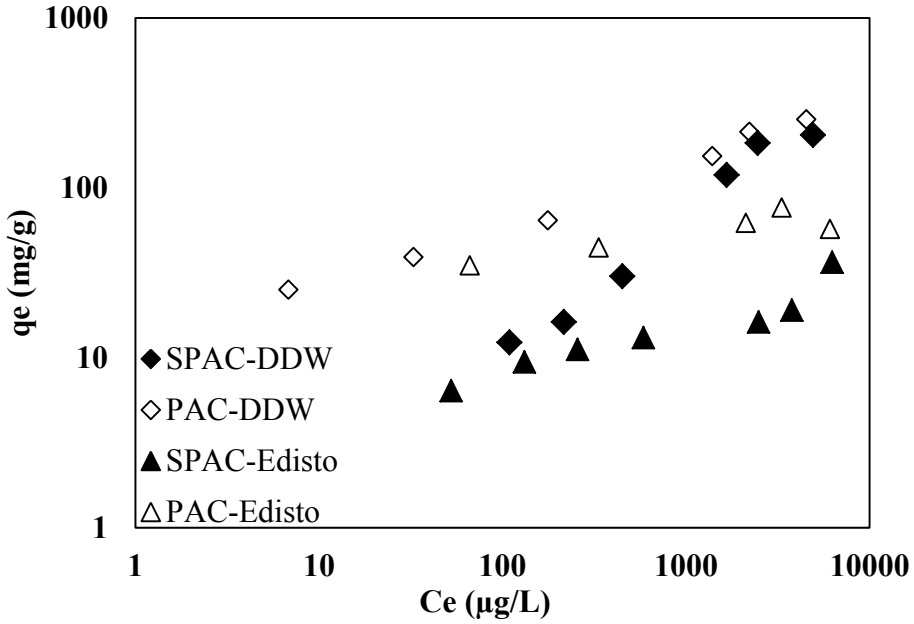

Figure 5.20 2PP adsorption isotherms for SPAC and PAC in DDW and Edisto River raw water with 4 mg DOC/L

Figure 5.21 compared to 4mg DOC/L and 10 mg DOC/L background solution effect on 2PP adsorption capacity. DOC concentration did not affect the competition mechanism on both SPAC and PAC, also $K_F^{U\&M}$ values for 4 mg DOC/L was similar to 10 mg DOC/L (Table 5.6), the reason might be the preparation of diluted NOM solution or heterogeneity of NOM compounds.

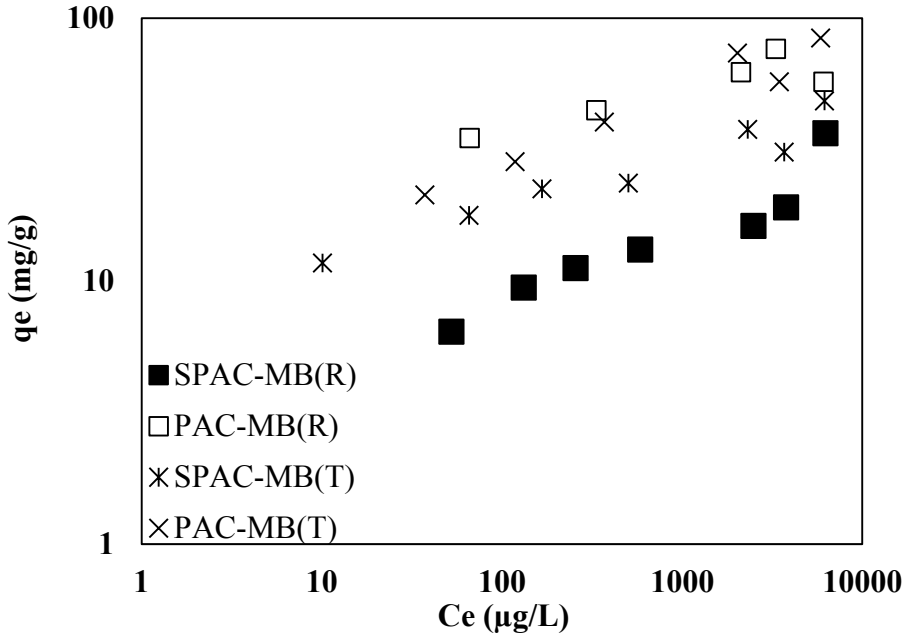

Figure 5.21 2PP adsorption isotherm in MB raw waters with 4 mg DOC/L and 10 mg DOC/L

Figure 5.22 compared the capacity of SPAC and PAC in low MW and high MW NOM. High MW NOM decreased 2PP adsorption capacity on SPAC more than low MW NOM. NOM with high MW might clog the macropores on SPAC surfaces and not let 2PP reach the pores.

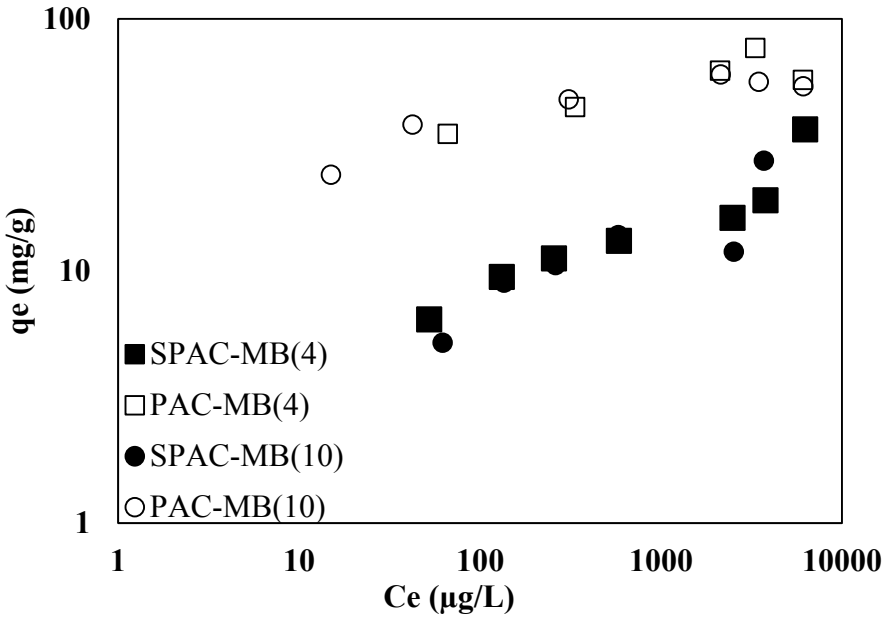

Figure 5.22 2PP adsorption isotherms in MB raw and treated waters with 4 mg DOC/L

Table 5.6 Nonlinear model fits of adsorption of 2PP on SPAC and PAC

ISOTHERMS		Freundlich				Langmuir			Polanyi-Manes			
		K_F^U μg/L	K_F^M mg/L	n	r^2	q_m	K_L	r^2	q_m	a	b	r^2
SPAC	DDW	0.32	69	0.78	0.975	339	0.000	0.973	257	-122840	5.6	0.992
	Edisto Raw=4mg DOC/L	3.2	15	0.23	0.697	39.3	0.002	0.865	4953	-4.94	0.3	0.51
	MB Raw= 4mg DOC/L	2.1	16	0.29	0.89	40	0.001	0.919	1764	-5.1	0.40	0.68
	MB Raw=10mgDOC/L	1.5	15	0.34	0.822	37	0.001	0.94	1723	-5.3	0.41	0.681
	MB Treated=4mg DOC/L	7.6	30	0.20	0.937	42	0.007	0.74	81	-7.1	1.2	0.834
PAC	DDW	11.2	142	0.37	0.989	295	0.001	0.95	2034	-10.2	0.96	0.992
	Edisto Raw=4mg DOC/L	15.5	45	0.16	0.889	55.9	0.024	0.765	8312	-3.84	0.233	0.878
	MB Raw=4mg DOC/L	20	53	0.15	0.786	65	0.013	0.701	72	-195	3.4	0.731
	MB Raw=10mgDOC/L	21	49	0.13	0.826	56	0.048	0.95	57	-18077	6.2	0.926
	MB Treated=4mg DOC/L	8.4	51	0.26	0.945	85	0.004	0.931	78710659	-8.4	0.13	0.955

K_F (L/μg): Freundlich adsorption affinity coefficient; n: nonlinear index; r^2: coefficient of determination; q_m (mg/g): maximum adsorption capacity; K_L (L/μg): Langmuir adsorption affinity coefficient; a and b: fitting parameters; underlined numbers represent the unreasonable values of PMM modeling.

5.5.1 2-Phenylphenol Adsorption Kinetics

2PP adsorption uptake rate in DDW and different NOM solutions were shown in Figure 5.23 to 5.25. It can be seen that PAC was significantly faster 2PP uptake rate than SPAC although NOM caused the reduction of rate in same extent SPAC and PAC. This result suggested that grinding did not effectively increase the 2PP adsorption kinetics in contrast to PNT, ATZ and CMZ kinetics also geosmin and MIB results in literature [16].

As mentioned, PAC was oxidized during grinding process. Oxidation also caused the disappearance of surface positive charge [82]. On the other hand, solutions pH (~6-7) was lower than pH_{PZC} values of SPAC and PAC (Table 5.2), which means carbon surface positively charge [83]. Also, if the decrease in the pH_{PZC} value was considered after crushing, it was clearly proved that surface positive charge was lost. Less positively charged carbon surfaces had less tendency to adsorb 2PP due to electron-donating behavior of –OH group. Moreover, as previously stated, oxygen and nitrogen functional groups impair the adsorption of organic compounds because they can serve as hydrogen-bond donor and/or acceptor sites which interact with water molecules more than SOCs [65]. Thus, formation of water clusters on hydrophilic SPAC prevented 2PP access the pores and reduce the interaction energy between 2PP and SPAC.

When we compared 2PP adsorption rate to CMZ, it was clearly seen that oxidized SPAC had more severe impact on 2PP rather than CMZ. Even if CMZ has electron donating group ($-NH_2$), it has also electron withdrawing groups (-C=O). However, -OH

functional group at –ortho position in 2PP had more effect on electrostatic interactions than $–NH_2$ in CMZ. Moreover, 2PP adsorption rate was slower than CMZ. Another factor can be the high solubility, larger third dimension of 2PP molecules and (-OH) group in its structure.

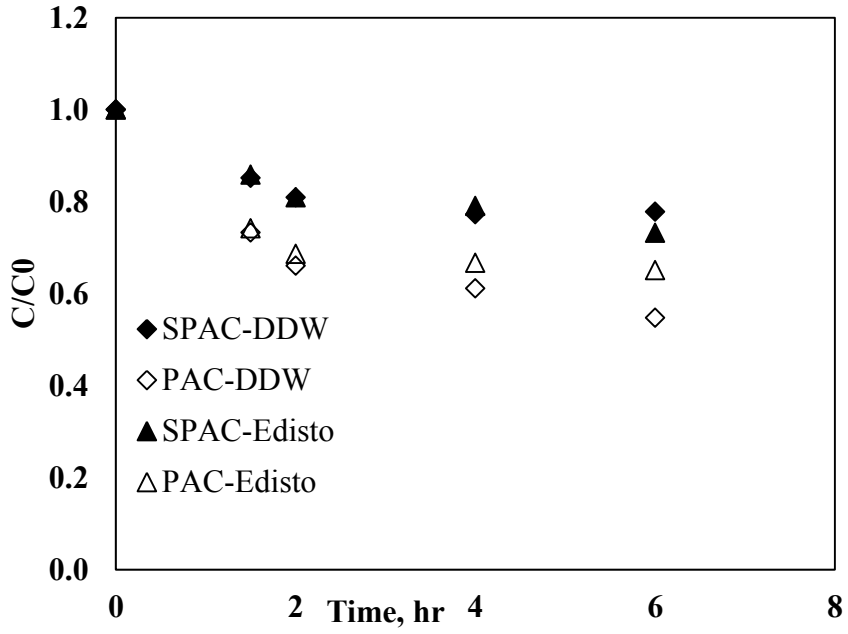

Figure 5.23 2PP adsorption kinetics for SPAC and PAC in DDW and Edisto River raw water with 4 mg DOC/L

The range of NOM concentration and MW effect on 2PP uptake rate was shown in Figure 5.24 and 5.25. It can be observed that NOM concentration and MW impact did not present strong competition effect on 2PP even if PAC had still faster adsorption kinetics on 2PP than SPAC.

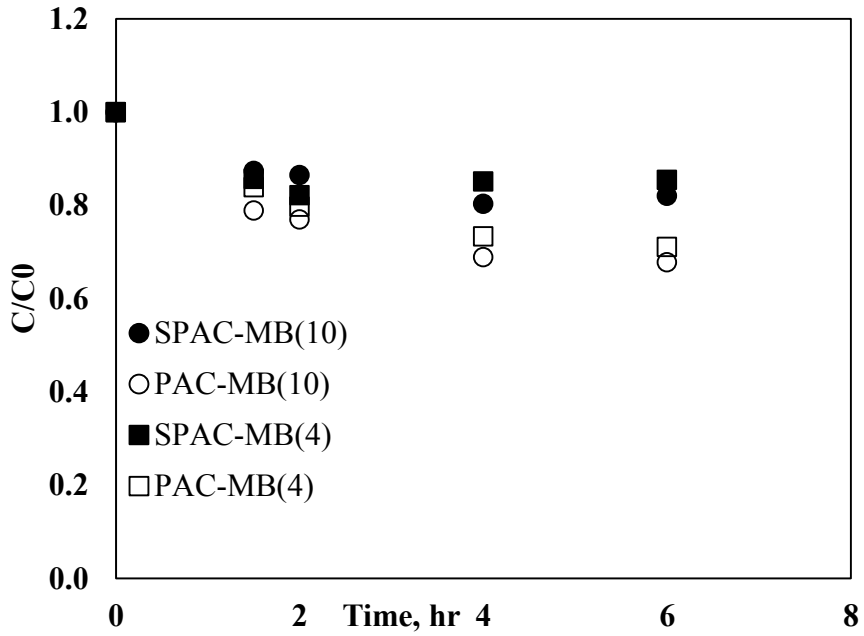

Figure 5.24 2PP adsorption kinetics in MB raw waters with 4 mg DOC/L and 10 mg DOC/L

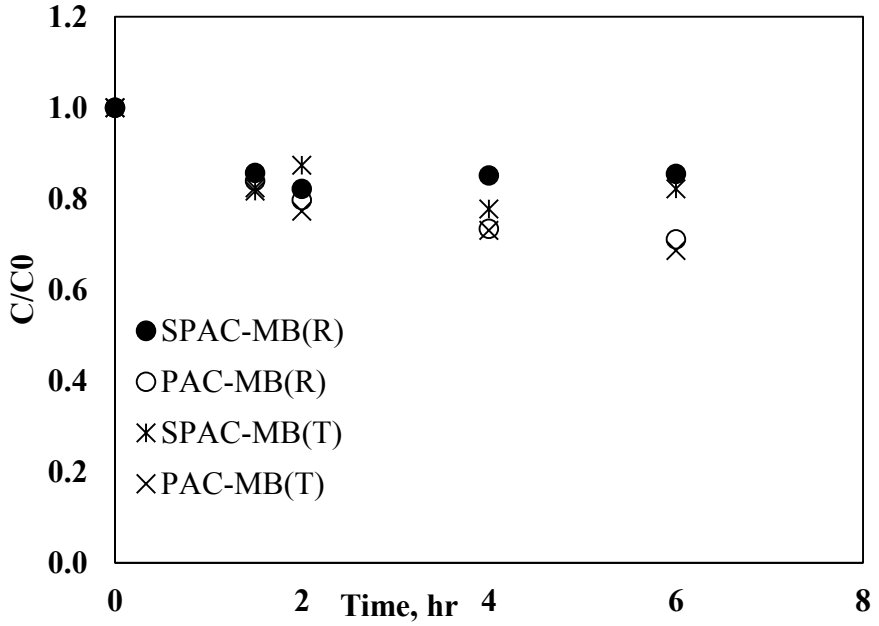

Figure 5.25 2PP adsorption kinetics in MB raw and treated waters with 4 mg DOC/L

5.6 Summary of SOCs Adsorption Capacity and Rate on SPAC & PAC

For all isotherms, the capacity of four compounds is higher for PAC than SPAC in DDW and NOM solutions. The higher capacity of PAC than SPAC is likely due to the higher microporosity of PAC than SPAC allowing better micropore filling and higher adsorption energies.

For kinetic experiments, adsorption rate of PNT, ATZ, CMZ during the first 6 hrs was faster on SPAC than PAC. However, the adsorption rate of PNT and ATZ was faster than CMZ which was attributed to the smaller size of PNT and ATZ than CMZ, and more external surface area and macroporous nature of SPAC than PAC allowing faster access of SOC molecules to carbon surface and pores. On the other hand, for 2PP adsorption kinetics, the rate of adsorption was slowest among all four SOCs and the SPAC did not show faster adsorption rate than PAC during the first six hours. This may results from multiple factors: (i) higher solubility of 2 PP, (ii) the larger third dimension as compared to other molecules, and (iii) the presence of an electron donating (-OH) group on its structure making the molecules slightly negative while increasing oxygen content of SPAC which increases the negative surface charge, overall negatively impacting the adsorption rate of 2PP. Therefore, the advantage of SPAC over PAC at the short contact times can be compound specific. The presence of NOM had a small impact on the adsorption rates of four SOC by SPAC during the first 6 hours contact time. The difference in the NOM characteristics (MB raw $SUVA_{254}$=4.4 and MB treated

$SUVA_{254}$=2.1, Edisto $SUVA_{254}$=2) and NOM concentrations (4 mg/L vs. 10 mg/L) did not seem to significantly impact the adsorption rates. The only exceptions were observed for atrazine.

Apart from all experiments done with Coal-based Watercarb (WC) 800 carbon, there was another type of PAC and its SPAC, which was Norit 20B carbon. However, after PNT and CMZ kinetic experiments done with that carbon showed that SPAC did not have advantage over PAC, it was decided to not use that carbon. The PNT and CMZ kinetic experiments result in DDW can be found in Figure A.11 and A.12.

5.7 Effect of Carbon Surface Oxidation on SOC Adsorption

To examine the impact of the carbon surface chemistry and water-adsorbent interactions on SOC adsorption, CMZ and 2PP isotherms were investigated with the PAC and oxidized surface SPAC. The major differences between SPAC and PAC were in their oxygen and nitrogen contents (Table 5.2), which were higher for the SPAC. As stated previously, the carbons with high oxygen and nitrogen content were more hydrophilic; therefore, their affinities for organic compounds were lower [65, 82]. Moreover, the oxidized activated carbons demonstrated higher affinities for water. Water clusters prevent the organic compound access to the basal planes of adsorbent/or reduce the interaction energy between compounds and the adsorbent surface [84].

On the other side, SOCs surface polarity also plays role for the adsorption on oxidized carbon surface. CMZ and 2PP was chosen to see the impact of π-π EDA on the

oxidized surface. The K_F of SOCs was plotted to the sum of the oxygen and nitrogen contents relative to surface area in Figure 5.26. As displayed there, K_F values decreased with increasing $(O+N)/S_{BET}$ rations indicated that a negative relationship existed between CMZ and 2PP distribution coefficients and polarity of adsorbents. The results confirmed the negative impact of the surface polarity and water cluster formation on the SOC adsorption. Especially, the decrease in K_F for 2PP was more intense than CMZ. Electron donor (-OH) functional group on 2PP was more negatively affected by oxidized surface than electron donor ($-NH_2$) and electron withdrawing (C=O) groups on CMZ. Because ATZ data was scattering and PNT does not have a functional group in its structure, CMZ and 2PP data were chosen for this analysis.

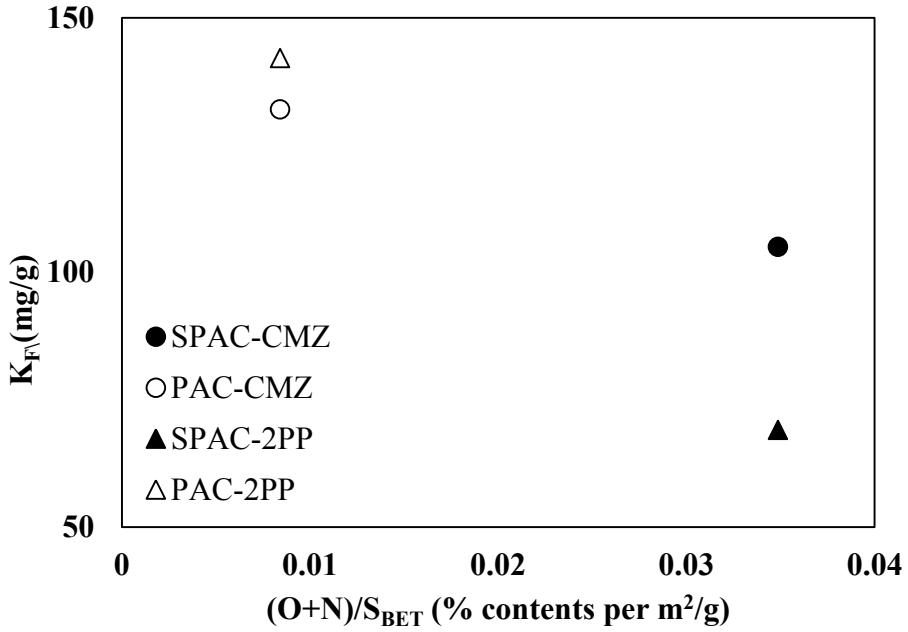

Figure 5.26 Relationship between Freundlich distribution coefficients of adsorbates and surface normalized O+N content of adsorbents.

5.8 Effect of SOC Properties on Adsorption

To analyze the SOCs properties on adsorption, solubility impact was investigated. PNT, CMZ and 2PP was chosen due to not only the large range of solubility differences but also similar molecular dimensions rather than ATZ whose first dimensions was lower than other three molecules. The K_F of SPAC relative to K_F of PAC was plotted to SOCs solubility in Figure 5.27. As seen, when the solubility was increased, adsorption capacity was decreased. If compound known with solubility is given, the approximate adsorption capacity on SPAC relative to PAC can be found.

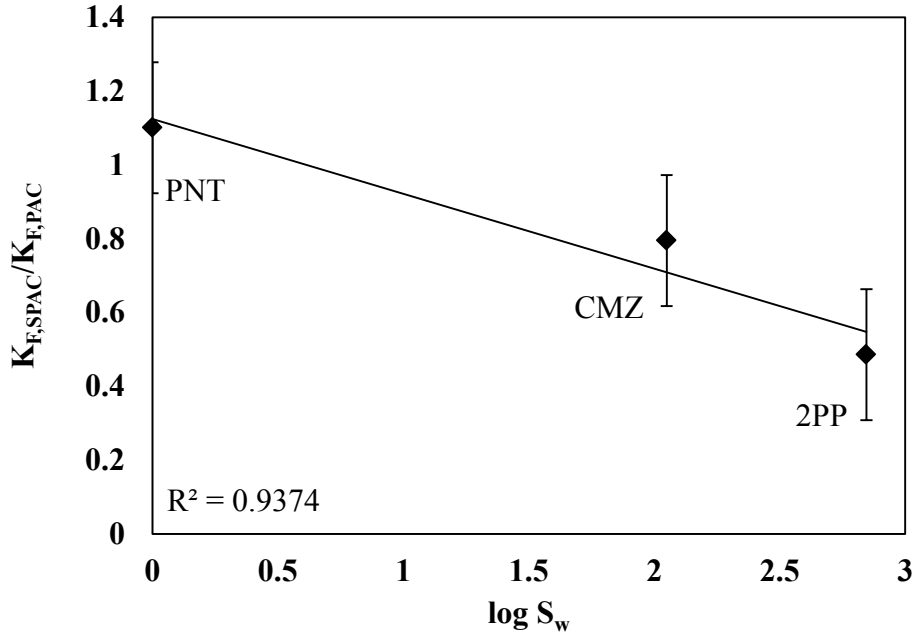

Figure 5.27 Correlation between the solubility of adsorbates and their relative adsorption capacities (Error bars indicated the 95% confidence interval)

CHAPTER 6

6 CONCLUSION AND RECOMMENDATION

The substantial conclusions obtained from this research were listed as following:

Objective 1: To understand the impact of crushing on carbon characteristics.

- Grinding the carbon caused the reduction in specific surface area even though particle size gets smaller and greater external surface area.
- BET surface area may not be only factor for adsorption behavior of SPAC and PAC.
- After grinding, micropore volume was decreased, and mesopore and macropore volume was increased.
- SPAC had higher nitrogen, oxygen and iron content than parent PAC due to crush with steel bead mill.
- Oxidized surface of SPAC might increase the more water molecule adsorption on surface. These water clusters caused the reduction of the available sorption sites.

Objective 2: To analyze adsorption behavior of SPAC and compare to PAC for four different SOC in both DDW and natural waters.

- In all background solutions, PAC adsorption capacity was slightly higher than SPAC.

- The smaller carbon particle size impact became less important as contact time was increased due to aggregation of SPAC particles and more water molecules adsorption on SPAC surface.
- PNT, ATZ and CMZ kinetics were faster with SPAC compared to PAC; however, 2PP showed the opposite behavior.
- The advantage of SPAC over PAC at the short contact times can be compound specific.
- NOM solution had small impact on PNT, CMZ and 2PP adsorption rates on SPAC and PAC during first 6 hours except ATZ.
- The difference in the NOM characteristics (MB raw $SUVA_{254}$=4.4 and MB treated $SUVA_{254}$=2.1, Edisto $SUVA_{254}$=2) and NOM concentrations (4 mg/L vs. 10 mg/L) did not seem to significantly impact the adsorption rates. The only exceptions were observed for atrazine, which is the smallest compound among four SOCs.
- In terms of surface chemistry of the carbons, hydrophobic carbon has stronger adsorption affinity to SOCs than its hydrophilic carbon.
- For each SOC, there was a specific pore size region depending on molecular dimensions. Pore volume of pores less than 1 nm was dominant site for ATZ, pores 1-2 nm were important for PNT, CMZ and 2PP, respectively.

***Objective 3*: To evaluate adsorption mechanism of different SOC properties on SPAC and PAC.**

- Functional groups on SOCs influenced the adsorption on oxidized surface which caused the disappearance of some positive charge.
- Electron donating functional groups such as $–NH_2$ and –OH may cause to reduction in electrostatic interaction between compound and oxidized carbon surface, whereas electron withdrawing groups (-Cl and C=O) enhanced the adsorption.
- Increased in solubility causes the decrease in adsorption capacity on both SPAC and PAC.
- Large molecules had slower intraparticle mass transfer rate.
- Smaller, planar compounds (PNT &ATZ) adsorbed faster and a greater extent than large, nonplanar and hydrophilic compounds (CMZ & 2PP).

Recommendations

- More carbons need to be tested.
- Because oxidation of carbon surfaces reduces interactions between adsorbate and adsorbent, it is important to analyze carbon characteristics before and after grinding process.

- In the future, it could be done some kind of chemical treatment, like acid application perhaps, to remove the iron hydroxide coming from milling process, or noniron mill can be used.
- These experiments can be performed for different particle size of carbons by selecting additional SOCs with different molecular size, solubility, molecular configuration and functional groups.
- Contact time is also critical to get advantage from small particle size. SPAC has superiority on adsorption in shorter contact time [85].
- Different background solutions, such as NOM at different pH, ionic strength effect or wastewater effluent organic matter can be used.

APPENDIX

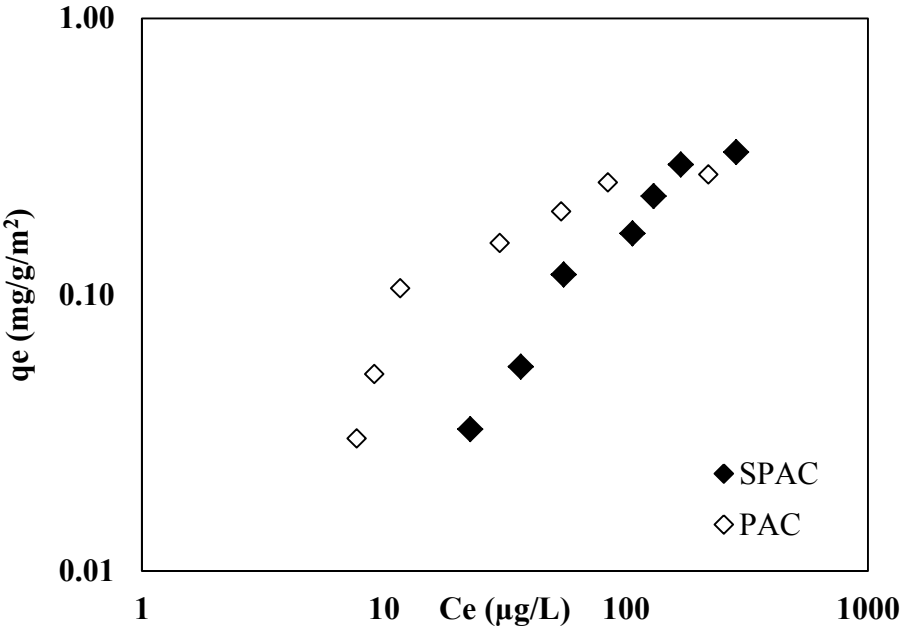

Figure A.1 PNT BET surface area normalization adsorption isotherm in DDW

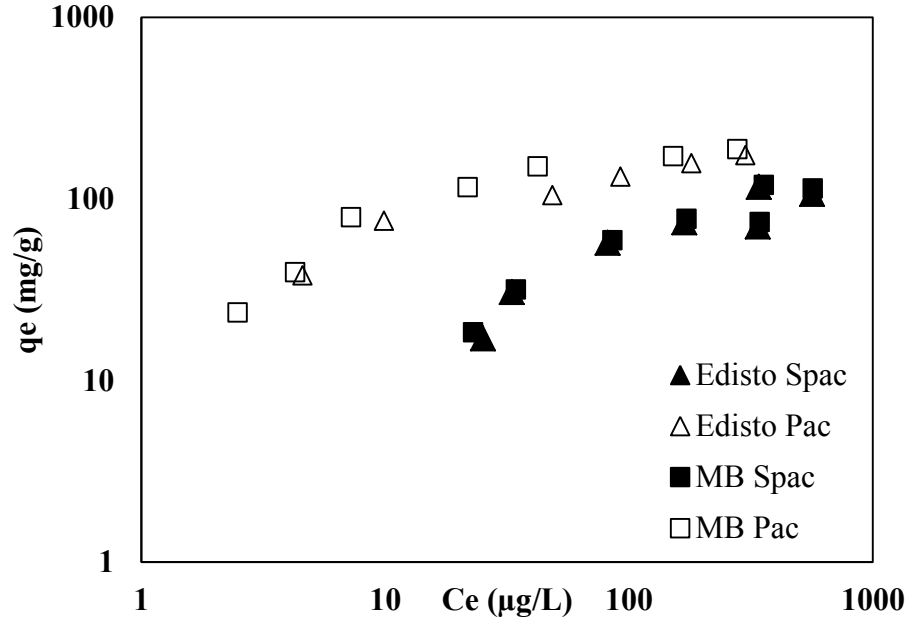

Figure A.2 PNT adsorption isotherm in different natural water at 4mg DOC/L

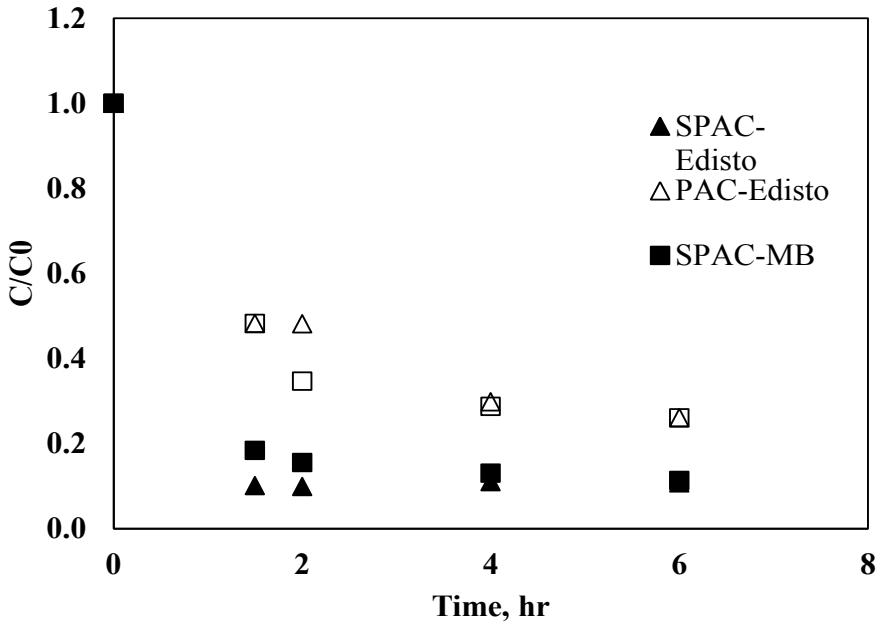

Figure A.3 PNT adsorption kinetics in different type of natural water at 4mg DOC/L

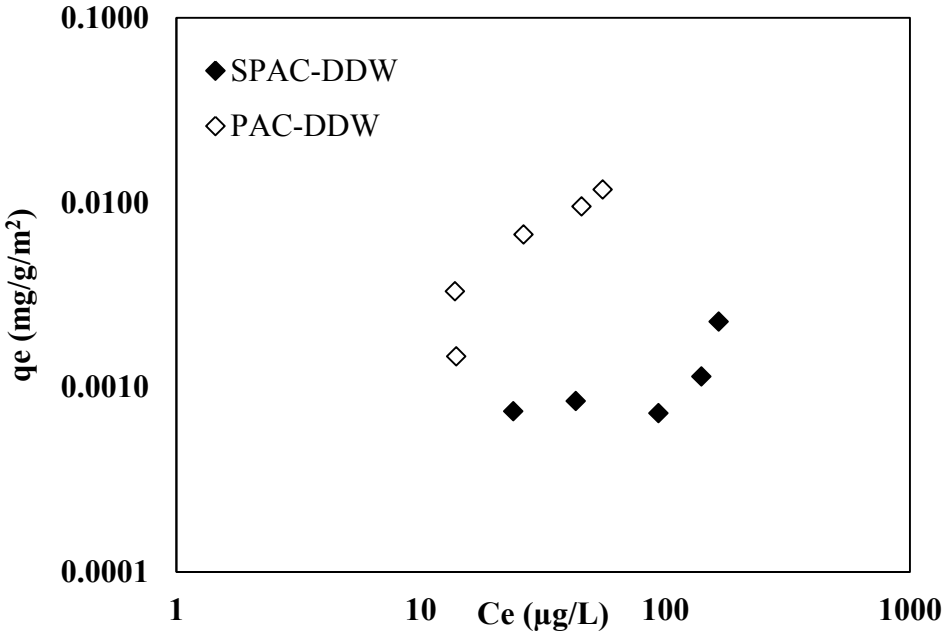

Figure A.4 ATZ BET surface area normalization adsorption isotherm in DDW

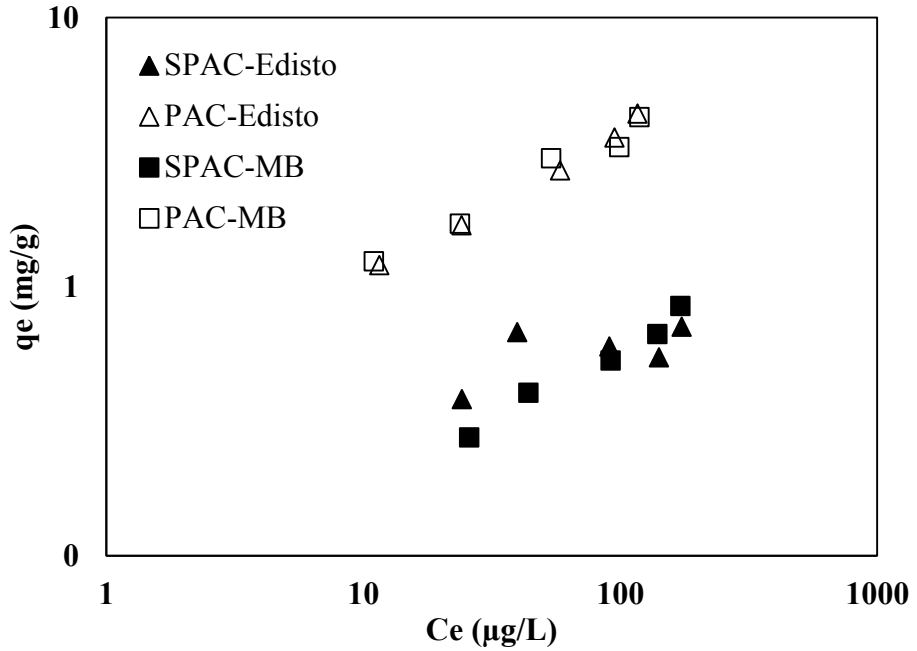

Figure A.5 ATZ adsorption isotherm in different type of natural water at 4mg DOC/L

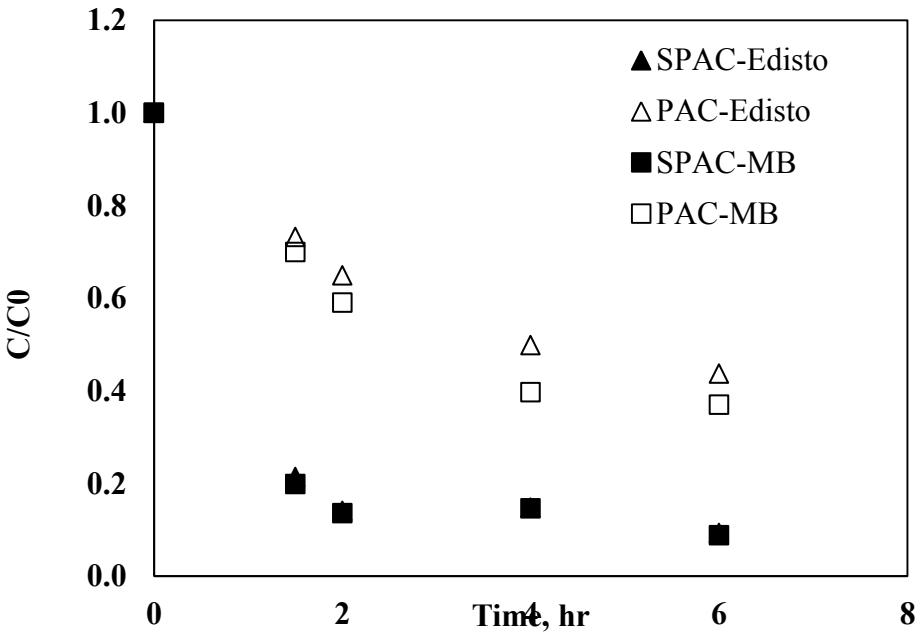

Figure A.6 ATZ adsorption kinetics in different type of natural water at 4mg DOC/L

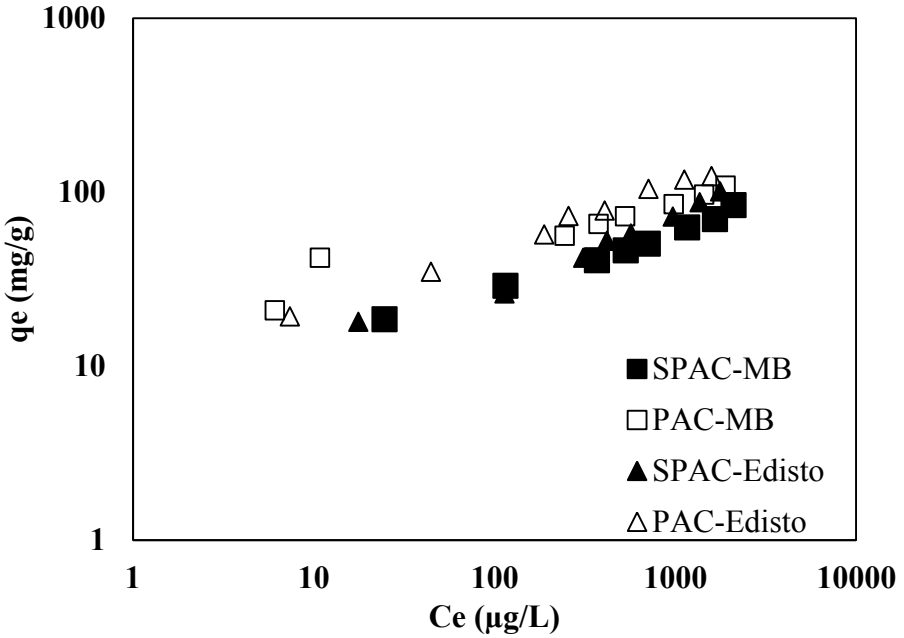

Figure A.7 CMZ adsorption isotherm in different type of natural water at 4mg DOC/L

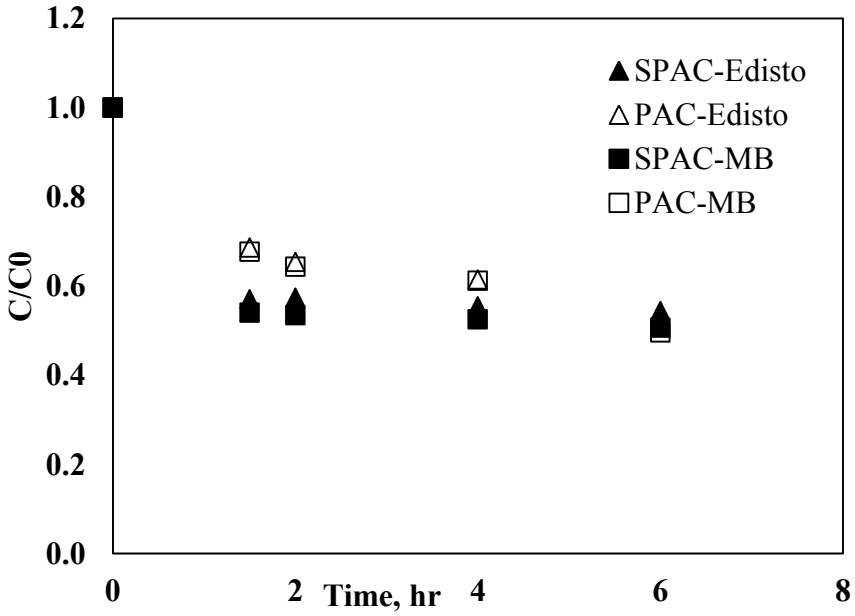

Figure A.8 CMZ adsorption kinetics in different type of natural water at 4mg DOC/L

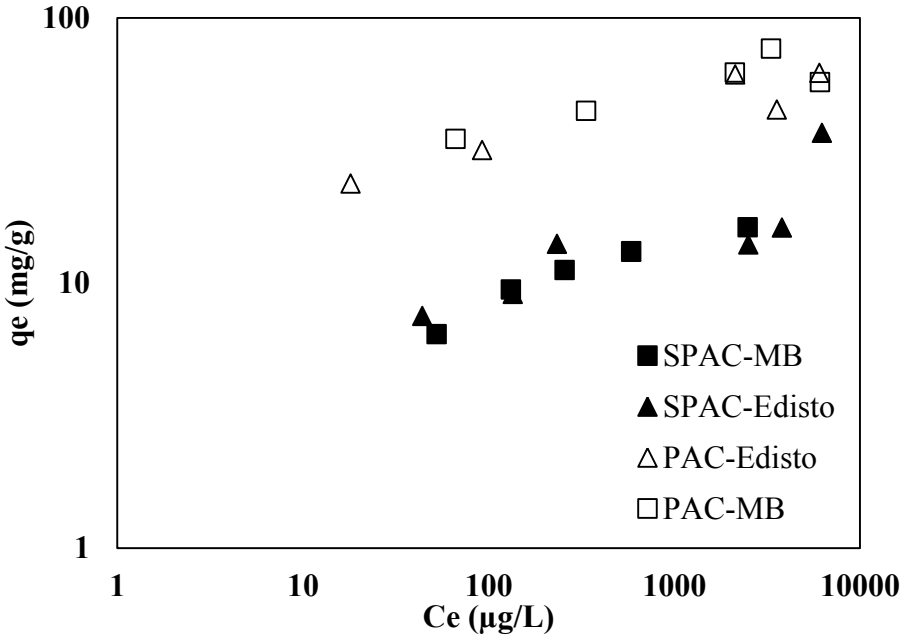

Figure A.9 2PP adsorption isotherm in different type of natural water at 4mg DOC/L

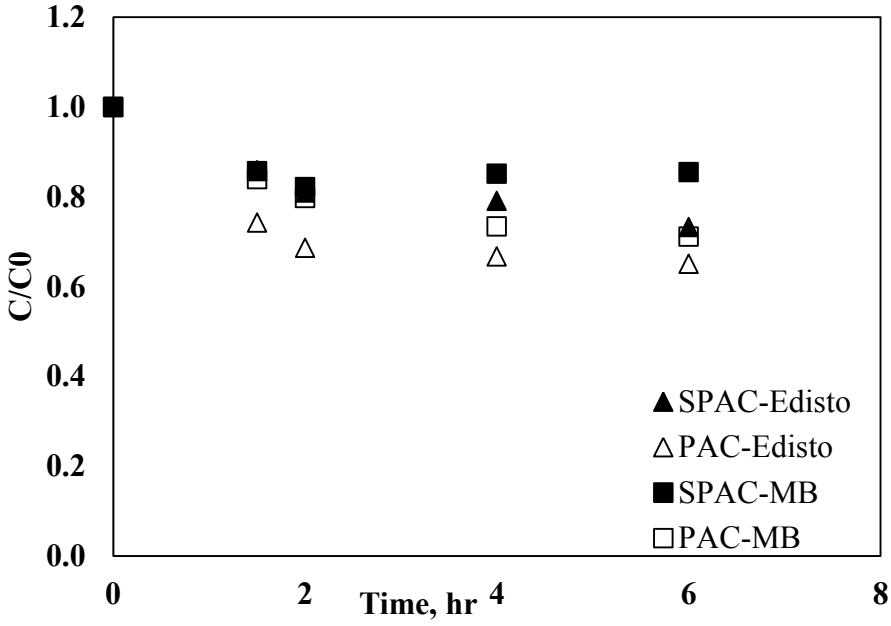

Figure A.10 2PP adsorption kinetics in different type of natural water at 4mg DOC/L

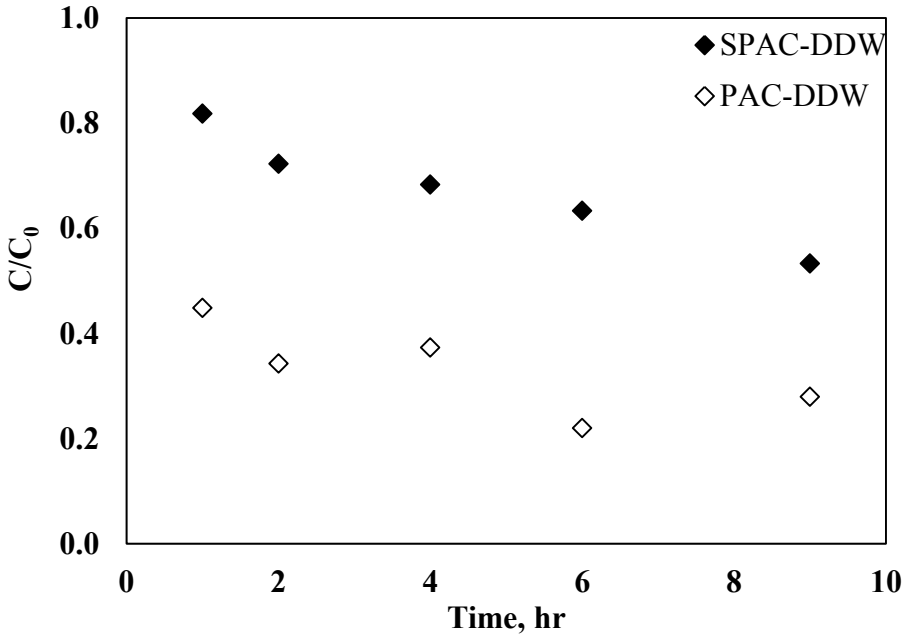

Figure A.11 PNT adsorption kinetics in DDW with Norit 20B carbon

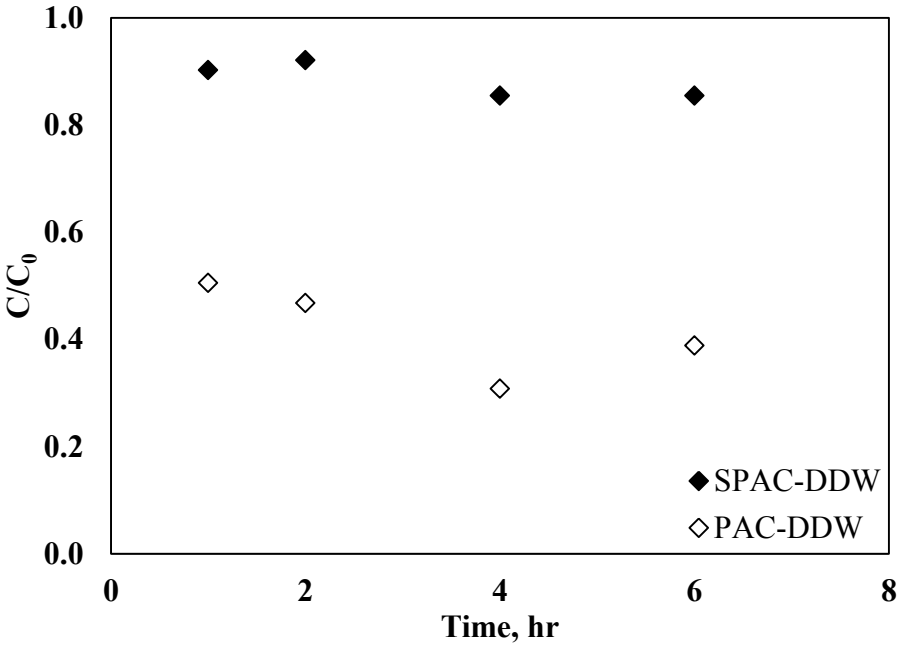

Figure A.12 CMZ adsorption kinetics in DDW with Norit 20B carbon

Table A.1 Ash Content of PAC and SPAC

Element		PAC	SPAC
P	%	0.15	0.12
K	%	0.052	0.056
Ca	%	1.54	0.86
Mg	%	0.38	0.31
Zn	%	0.16	0.14
Cu	%	0.003	0.045
Mn	%	0.026	0.12
Fe	%	0.41	15.5
S	%	0.32	0.23
Na	%	0.077	0.077
B	%	0.006	0.005
Al	%	0.49	0.6

REFERENCES

1. Dąbrowski, A., P. Podkościelny, Z. Hubicki, and M. Barczak, *Adsorption of phenolic compounds by activated carbon—a critical review.* Chemosphere, 2005. **58**(8): p. 1049-1070.

2. Delgado, L.F., P. Charles, K. Glucina, and C. Morlay, *The removal of endocrine disrupting compounds, pharmaceutically activated compounds and cyanobacterial toxins during drinking water preparation using activated carbon—A review.* Science of The Total Environment, 2012. **435**: p. 509-525.

3. Heo, J., L.K. Boateng, J.R.V. Flora, H. Lee, N. Her, Y.-G. Park, and Y. Yoon, *Comparison of flux behavior and synthetic organic compound removal by forward osmosis and reverse osmosis membranes.* Journal of Membrane Science, 2013. **443**(0): p. 69-82.

4. USEPA, *Safe Drinking Water Act.* 1986.

5. USEPA. *Safe Drinking Water Act*. 2007; Available from: www.epa.gov/safewater/sdwa/index.html.

6. Macdonald, R.W., L.A. Barrie, T.F. Bidleman, M.L. Diamond, D.J. Gregor, R.G. Semkin, M.B. Yunker, *Contaminants in the Canadian Arctic: 5 years of progress in understanding sources, occurrence and pathways.* Science of The Total Environment, 2000. **254**(2–3): p. 93-234.

7. Karanfil, T., S.A. Dastgheib, and D. Mauldin, *Exploring molecular sieve capabilities of activated carbon fibers to reduce the impact of NOM preloading on trichloroethylene adsorption.* Environmental science & technology, 2006. **40**(4): p. 1321-1327.

8. Focazio, M.J., D.W. Kolpin, K.K. Barnes, E.T. Furlong, M.T. Meyer, S.D. Zaugg, M.E. Thurman, *A national reconnaissance for pharmaceuticals and other organic wastewater contaminants in the United States — II) Untreated drinking water sources.* Science of The Total Environment, 2008. **402**(2–3): p. 201-216.

9. Matsui, Y., T. Aizawa, F. Kanda, N. Nigorikawa, S. Mima, and Y. Kawase, *Adsorptive removal of geosmin by ceramic membrane filtration with super-powdered activated carbon.* Journal of Water Supply: Research and Technology, AQUA, 2007. **56**(6–7): p. 411-418.

10. Ando, N., Y. Matsui, R. Kurotobi, Y. Nakano, T. Matsushita, and K. Ohno, *Comparison of natural organic matter adsorption capacities of super-powdered activated carbon and powdered activated Carbon.* Water Research, 2010. **44**(14): p. 4127-4136.

11. Mangun, C.L., K.R. Benak, J. Economy, and K.L. Foster, *Surface chemistry, pore sizes and adsorption properties of activated carbon fibers and precursors treated with ammonia.* Carbon, 2001. **39**(12): p. 1809-1820.

12. Cheng, W., S.A. Dastgheib, and T. Karanfil, *Adsorption of dissolved natural organic matter by modified activated carbons.* Water Research, 2005. **39**(11): p. 2281-2290.

13. Zhang, S., T. Shao, and T. Karanfil, *The effects of dissolved natural organic matter on the adsorption of synthetic organic chemicals by activated carbons and carbon nanotubes.* Water Research, 2011. **45**(3): p. 1378-1386.

14. Kilduff, J.E., T. Karanfil, and W.J. Weber Jr, *Competitive effects of nondisplaceable organic compounds on trichloroethylene uptake by activated carbon. II. Model verification and applicability to natural organic matter.* Journal of colloid and interface science, 1998. **205**(2): p. 280-289.

15. Newcombe, G., M. Drikas, and R. Hayes, *Influence of characterised natural organic material on activated carbon adsorption: II. Effect on pore volume distribution and adsorption of 2-methylisoborneol.* Water Research, 1997. **31**(5): p. 1065-1073.

16. Matsui, Y., Y. Nakano, H. Hiroshi, N. Ando, T. Matsushita, and K. Ohno, *Geosmin and 2-methylisoborneol adsorption on super-powdered activated carbon in the presence of natural organic matter.* 2010.

17. Choma, J. and M. Jaroniec, *Characterization of nanoporous carbons by using gas adsorption isotherms.* Interface Science and Technology, 2006. **7**: p. 107-158.

18. Marsh, H. and F.R. Reinoso, *Activated carbon*. 2006: Elsevier.

19. Menendez-Diaz, J. and I. Martin-Gullon, *Types of carbon adsorbents and their production.* Interface Science and Technology, 2006. **7**: p. 1-47.

20. Bansal, R.C. and M. Goyal, *Activated carbon adsorption*. 2010: CRC press.

21. Norley, J. *The Role of Natural Graphite in Electronics Cooling*. 2001 [cited March 2014; Available from: http://www.electronics-cooling.com/2001/08/the-role-of-natural-graphite-in-electronics-cooling/.

22. Lastoskie, C., K.E. Gubbins, and N. Quirke, *Pore size distribution analysis of microporous carbons: a density functional theory approach.* The journal of physical chemistry, 1993. **97**(18): p. 4786-4796.

23. Pelekani, C. and V. Snoeyink, *Competitive adsorption in natural water: role of activated carbon pore size.* Water Research, 1999. **33**(5): p. 1209-1219.

24. Hopman, R., W. Siegers, and J. Kruithof, *Organic micropollutant removal by activated carbon fiber filtration.* Water Supply[WATER SUPPLY]. 1995. **13**(3-4).

25. Karanfil, T., M. Kitis, J.E. Kilduff, and A. Wigton, *Role of granular activated carbon surface chemistry on the adsorption of organic compounds. 2. Natural organic matter.* Environmental science & technology, 1999. **33**(18): p. 3225-3233.

26. Kose, H.S., *The Effects of Physical Factors on the Adsorption of Synthetic Organic Compounds by Activated Carbon and Activated Carbon Fibers*. 2010, Clemson University.

27. Bandosz, T.J., *Activated carbon surfaces in environmental remediation*. Vol. 7. 2006: Academic Press.

28. Weber Jr, W.J., T.C. Voice, and A. Jodellah, *Adsorption of humic substances: the effects of heterogeneity and system characteristics.* Journal-American Water Works Association, 1983. **75**(12): p. 612-619.

29. Matsui, Y., Y. Fukuda, R. Murase, N. Aoki, S. Mima, T. Inoue, and T. Matsushita. *Ceramic MF with Submicron-sized Activated Carbon Adsorption and Coagulation Pretreatments for Rapid and Effective NOM Removal*. in *2nd IWA Leading-Edge Conference on Water and Wastewater Treatment Technologies*. 2004: IWA Publishing.

30. Matsui, Y., R. Murase, T. Sanogawa, N. Aoki, S. Mima, T. Inoue, and T. Matsushita, *Rapid adsorption pretreatment with submicrometre powdered activated carbon particles before microfiltration.* Water Science & Technology, 2005. **51**(6-7): p. 249-256.

31. Ellerie, J.R., *Carbonaceous adsorbents as coatings for ultrafiltration membranes.*, in *Environmental engineering and Science*. 2012, Clemson University: Anderson. p. 113.

32. Dunn, S., *Effect of Powdered Activated Carbon Base Material and Size on Disinfection By-Product Precursor and Trace Organic Pollutant Removal.* 2011.

33. Matsui, Y., R. Murase, T. Sanogawa, N. Aoki, S. Mima, T. Inoue, and T. Matsushita, *Micro-ground powdered activated carbon for effective removal of natural organic matter during water treatment.* Water Supply, 2004. **4**(4): p. 155-163.

34. Ellerie, J.R., O.G. Apul, T. Karanfil, and D.A. Ladner, *Comparing graphene, carbon nanotubes, and superfine powdered activated carbon as adsorptive coating materials for microfiltration membranes.* Journal of Hazardous Materials, 2013. **261**(0): p. 91-98.

35. Matsui, Y., Y. Fukuda, T. Inoue, and T. Matsushita, *Effect of natural organic matter on powdered activated carbon adsorption of trace contaminants: characteristics and mechanism of competitive adsorption.* Water Research, 2003. **37**(18): p. 4413-4424.

36. Matsui, Y., N. Ando, T. Yoshida, R. Kurotobi, T. Matsushita, and K. Ohno, *Modeling high adsorption capacity and kinetics of organic macromolecules on super-powdered activated carbon.* Water Research, 2011. **45**(4): p. 1720-1728.

37. Ando, N., Y. Matsui, T. Matsushita, and K. Ohno, *Direct observation of solid-phase adsorbate concentration profile in powdered activated carbon particle to elucidate mechanism of high adsorption capacity on super-powdered activated carbon.* Water Research, 2011. **45**(2): p. 761-767.

38. Letterman, R.D., J. Quon, and R.S. Gemmell, *Film transport coefficient in agitated suspensions of activated carbon.* Journal (Water Pollution Control Federation), 1974: p. 2536-2546.

39. Matsui, Y., T. Yoshida, S. Nakao, D.R.U. Knappe, and T. Matsushita, *Characteristics of competitive adsorption between 2-methylisoborneol and natural organic matter on superfine and conventionally sized powdered activated carbons.* Water Research, 2012. **46**(15): p. 4741-4749.

40. Stavropoulos, G., P. Samaras, and G. Sakellaropoulos, *Effect of activated carbons modification on porosity, surface structure and phenol adsorption.* Journal of Hazardous Materials, 2008. **151**(2): p. 414-421.

41. Matsui, Y., Y. Nakano, H. Hiroshi, N. Ando, T. Matsushita, and K. Ohno, *Geosmin and 2-methylisoborneol adsorption on super-powdered activated carbon in the presence of natural organic matter.* Water Sci Technol, 2010. **62**(11): p. 2664-8.

42. Ellerie, J.R., O.G. Apul, T. Karanfil, and D.A. Ladner, *Comparing graphene, carbon nanotubes, and superfine powdered activated carbon as adsorptive coating materials for microfiltration membranes.* J Hazard Mater, 2013. **261C**: p. 91-98.

43. Hamad, J., M. Kennedy, B. Hofs, S. Heijman, and G. Amy, *SUPER GROUND PAC IN COMBINATION WITH CERAMIC.* Journal of Sciences, Islamic Republic of Iran, 2002. **13**(3): p. 241-247.

44. Matsui, Y., S. Nakao, T. Taniguchi, and T. Matsushita, *Geosmin and 2-methylisoborneol removal using superfine powdered activated carbon: Shell adsorption and branched-pore kinetic model analysis and optimal particle size.* Water Research, 2013. **47**(8): p. 2873-2880.

45. Matsui, Y., N. Ando, H. Sasaki, T. Matsushita, and K. Ohno, *Branched pore kinetic model analysis of geosmin adsorption on super-powdered activated carbon.* Water Research, 2009. **43**(12): p. 3095-3103.

46. Jia, Q. and A.C. Lua, *Concentration-dependent branched pore kinetic model for aqueous phase adsorption.* Chemical Engineering Journal, 2008. **136**(2–3): p. 227-235.

47. Peel, R.G., A. Benedek, and C.M. Crowe, *A branched pore kinetic model for activated carbon adsorption.* AIChE Journal, 1981. **27**(1): p. 26-32.

48. Dudley, L.-A.L., A. ; Strynar, M. ; McMillan, L. ; Knappe, D.R.E. ; American Water Works Association, *Removal of Perfluorinated Compounds by Powdered Activated Carbon: Effects of Adsorbent and Background Water Characteristics*. 2012, Annual Conference And Exposition - American Water Works Association; 2; 961-1003

49. Matsui, Y., S. Nakao, T. Yoshida, T. Taniguchi, and T. Matsushita, *Natural organic matter that penetrates or does not penetrate activated carbon and competes or does not compete with geosmin.* Separation and Purification Technology, 2013.

50. Quinlivan, P.A., L. Li, and D.R.U. Knappe, *Effects of activated carbon characteristics on the simultaneous adsorption of aqueous organic micropollutants and natural organic matter.* Water Research, 2005. **39**(8): p. 1663-1673.

51. Li, L., P.A. Quinlivan, and D.R. Knappe, *Effects of activated carbon surface chemistry and pore structure on the adsorption of organic contaminants from aqueous solution.* Carbon, 2002. **40**(12): p. 2085-2100.

52. Karanfil, T. and J.E. Kilduff, *Role of granular activated carbon surface chemistry on the adsorption of organic compounds. 1. Priority pollutants.* Environmental science & technology, 1999. **33**(18): p. 3217-3224.

53. Radovic, L., I. Silva, J. Ume, J. Menendez, C. Leon, and A. Scaroni, *An experimental and theoretical study of the adsorption of aromatics possessing electron-withdrawing and electron-donating functional groups by chemically modified activated carbons.* Carbon, 1997. **35**(9): p. 1339-1348.

54. Coughlin, R.W., F.S. Ezra, and R.N. Tan, *Influence of chemisorbed oxygen in adsorption onto carbon from aqueous solution.* Journal of colloid and interface science, 1968. **28**(3): p. 386-396.

55. Garcıa, T., R. Murillo, D. Cazorla-Amoros, A. Mastral, and A. Linares-Solano, *Role of the activated carbon surface chemistry in the adsorption of phenanthrene.* Carbon, 2004. **42**(8): p. 1683-1689.

56. Menéndez, J.A., J. Phillips, B. Xia, and L.R. Radovic, *On the modification and characterization of chemical surface properties of activated carbon: in the search of carbons with stable basic properties.* Langmuir, 1996. **12**(18): p. 4404-4410.

57. Franz, M., H.A. Arafat, and N.G. Pinto, *Effect of chemical surface heterogeneity on the adsorption mechanism of dissolved aromatics on activated carbon.* Carbon, 2000. **38**(13): p. 1807-1819.

58. Pignatello, J.J. and B. Xing, *Mechanisms of slow sorption of organic chemicals to natural particles.* Environmental science & technology, 1995. **30**(1): p. 1-11.

59. Cornelissen, G., M. Elmquist, I. Groth, and Ö. Gustafsson, *Effect of sorbate planarity on environmental black carbon sorption.* Environmental science & technology, 2004. **38**(13): p. 3574-3580.

60. Jonker, M.T. and F. Smedes, *Preferential sorption of planar contaminants in sediments from Lake Ketelmeer, The Netherlands.* Environmental science & technology, 2000. **34**(9): p. 1620-1626.

61. Jonker, M.T. and A.A. Koelmans, *Polyoxymethylene solid phase extraction as a partitioning method for hydrophobic organic chemicals in sediment and soot.* Environmental science & technology, 2001. **35**(18): p. 3742-3748.

62. Jonker, M.T. and A.A. Koelmans, *Sorption of polycyclic aromatic hydrocarbons and polychlorinated biphenyls to soot and soot-like materials in the aqueous environment: mechanistic considerations.* Environmental science & technology, 2002. **36**(17): p. 3725-3734.

63. Guo, Y., A. Yadav, and T. Karanfil, *Approaches to mitigate the impact of dissolved organic matter on the adsorption of synthetic organic contaminants by porous carbonaceous sorbents.* Environmental science & technology, 2007. **41**(22): p. 7888-7894.

64. Kaneko, Y., M. Abe, and K. Ogino, *Adsorption characteristics of organic compounds dissolved in water on surface-improved activated carbon fibres.* Colloids and Surfaces, 1989. **37**: p. 211-222.

65. Karanfil, T. and S.A. Dastgheib, *Trichloroethylene adsorption by fibrous and granular activated carbons: aqueous phase, gas phase, and water vapor adsorption studies.* Environmental science & technology, 2004. **38**(22): p. 5834-5841.

66. Deryło-Marczewska, A., J. Goworek, A. Świątkowski, and B. Buczek, *Influence of differences in porous structure within granules of activated carbon on adsorption of aromatics from aqueous solutions.* Carbon, 2004. **42**(2): p. 301-306.

67. Villacañas, F., M.F.R. Pereira, J.J. Órfão, and J.L. Figueiredo, *Adsorption of simple aromatic compounds on activated carbons.* Journal of colloid and interface science, 2006. **293**(1): p. 128-136.

68. Ania, C., B. Cabal, J. Parra, A. Arenillas, B. Arias, and J. Pis, *Naphthalene adsorption on activated carbons using solvents of different polarity.* Adsorption, 2008. **14**(2-3): p. 343-355.

69. Dowaidar, A., M. El‐Shahawi, and I. Ashour, *Adsorption of Polycyclic Aromatic Hydrocarbons onto Activated Carbon from Non‐Aqueous Media: 1. The Influence of the Organic Solvent Polarity.* Separation Science and Technology, 2007. **42**(16): p. 3609-3622.

70. Weber, W.J. and B.M.v. Vliet, *Fundamental concepts for application of activated carbon in water and wastewater treatment*, in *Activated carbon adsorption of organics from the aqueous phase*. 1981, Ann Arbor Science. p. 15-41.

71. Pelekani, C. and V.L. Snoeyink, *Competitive adsorption between atrazine and methylene blue on activated carbon: the importance of pore size distribution.* Carbon, 2000. **38**(10): p. 1423-1436.

72. Kilduff, J.E., T. Karanfil, and W.J. Weber, *TCE adsorption by GAC preloaded with humic substances.* Journal-American Water Works Association, 1998. **90**(5): p. 76-89.

73. Kilduff, J.E. and T. Karanfil, *Trichloroethylene adsorption by activated carbon preloaded with humic substances: effects of solution chemistry.* Water Research, 2002. **36**(7): p. 1685-1698.

74. Matsui, Y., T. Yoshida, S. Nakao, D.R. Knappe, and T. Matsushita, *Characteristics of competitive adsorption between 2-methylisoborneol and natural organic matter on superfine and conventionally sized powdered activated carbons.* Water Research, 2012. **46**(15): p. 4741-4749.

75. Weber, W.J., *Physicochemical processes for water quality control*. 1972: Wiley Interscience.

76. Pikaar, I., A.A. Koelmans, and P. van Noort, *Sorption of organic compounds to activated carbons. Evaluation of isotherm models.* Chemosphere, 2006. **65**(11): p. 2343-2351.

77. Carter, M.C. and W.J. Weber, *Modeling adsorption of TCE by activated carbon preloaded by background organic matter.* Environmental science & technology, 1994. **28**(4): p. 614-623.

78. Chiou, C.C. and M. Manes, *Application of the Polanyi adsorption potential theory to adsorption from solution on activated carbon. V. Adsorption from water of some solids and their melts, and a comparison of bulk and adsorbate melting points.* The journal of physical chemistry, 1974. **78**(6): p. 622-626.

79. Greenbank, M. and M. Manes, *Application of the Polanyi adsorption potential theory to adsorption from solution on activated carbon. 11. Adsorption of organic liquid mixtures from water solution.* The journal of physical chemistry, 1981. **85**(21): p. 3050-3059.

80. Welham, N.J. and J.S. Williams, *Extended milling of graphite and activated carbon.* Carbon, 1998. **36**(9): p. 1309-1315.

81. Pelekani, C. and V.L. Snoeyink, *A kinetic and equilibrium study of competitive adsorption between atrazine and Congo red dye on activated carbon: the importance of pore size distribution.* Carbon, 2001. **39**(1): p. 25-37.

82. Cheng, C.-H., J. Lehmann, and M.H. Engelhard, *Natural oxidation of black carbon in soils: Changes in molecular form and surface charge along a climosequence.* Geochimica et Cosmochimica Acta, 2008. **72**(6): p. 1598-1610.

83. Summers, R.S. and P.V. Roberts, *Activated carbon adsorption of humic substances: II. Size exclusion and electrostatic interactions.* Journal of colloid and interface science, 1988. **122**(2): p. 382-397.

84. Zhang, W., Q.G. Chang, W.D. Liu, B.J. Li, W.X. Jiang, L.J. Fu, and W.C. Ying, *Selecting activated carbon for water and wastewater treatability studies.* Environmental Progress, 2007. **26**(3): p. 289-298.

85. Li, M., *Effects Of Natural Organic Matter On Contaminant Removal By Superfine Powdered Activated Carbon Coupled With Microfiltration Membranes*. 2014, Clemson University.